Table 7. Precipitation variation according to RCP8.5 scenario for the period 2016-2035

District	Rainfall change (%)
Phan Thiet	10.3
La Gi	6.2
Tuy Phong	6.0
Bac Binh	0.0
Ham Thuan Bac	-0.5
Ham Thuan Nam	2.0
Tanh Linh	3.1
Ham Tan	13.3
Duc Linh	2.6

Power production: climate change may lead to increase costs for power production activities during operation, cooling and maintenance. In addition, electric poles, transformer stations, power transmission lines, etc. are overloaded, degraded, damaged due to rising temperatures, rain, extreme climate; prolonged flooding can be dangerous due to electrical leakage.

Seafood processing: changes in temperature and precipitation would impacts on marine ecosystems, loss of diversity and reduction of seafood exploited for processing.

Mineral exploitation and processing: Heavy rain can cause underground mines of titanium to be flooded, makes the equipment damaged. Heavy rain also is likely to break pits, spill ore and make environmental incidents.

Factories, industrial clusters, traditional craft villages: Roads may be flooded due to heavy and prolonged rain. Heavy rain and prolonged heat could affect the manual production of traditional villages and reduce the number of tourists coming here. Temperature increases, prolonged heat is likely to make fire risk.

Trade centres, supermarkets, markets, petroleum stores, warehouses: Increasing temperature negatively tends to affects the sustainability of buildings, increase electricity consumption and raise cooling costs in trade centres, supermarkets and markets, respectively. The rise in temperature may increases the risk of fire in petroleum stores and warehouses.

Acknowledgement: *This study was carried out and completed thanks to the support of the project Developing action plans to respond to climate change for construction, transportation, industry and tourism sectors and districts in Binh Thuan province*

References

1. Department of Planning and Investment, (2017), *Project "Integrated management of water resources and urban development in relation to climate change in Binh Thuan".*
2. Department of Industry and Trade, (2017), *Report on implementation of 2017 tasks and orientation for 2018 of Industry and Trade sector.*
3. Department of Industry and Trade, (2012), *Development planning for Industry and Trade in Binh Thuan province to 2020, vision to 2030.*
4. Ministry of Natural Resources and Environment, (2016), *Update results of climate change, sea level rise scenarios for Viet Nam.*
5. Ministry of Industry and Trade, (2010), *Ministry of Industry and Trade's Action Plan to Respond to Climate Change.*
6. 6 Ministry of Industry and Trade, (2010), *Green growth action plan of Industry and Trade sector in the period of 2015-2020.*

IMPACT OF ENSO ON WATER DISCHARGE AND SEDIMENT LOAD IN LOWER MEKONG RIVER

Dang Thi Ha
School of Maritime Economics and Technology, Ba Ria - Vung Tau University

Received: 3 November 2018; Accepted 25 December 2018

Abstract: *The Mekong River is the second largest river basin in Southeast Asia and strongly influenced by climate change. This paper was based on high temporal resolution of water discharge and suspended sediment concentration at Can Tho and My Thuan stations during the 2009-2016 period, showed that the water discharge and sediment supplies by the Mekong strongly varied, and influenced by ENSO events (El Nino Southern Oscillation). Our results obtained showed that during the La Niña event (2010-2011), water supply increased by about 30% and the sediment supply by 55%. In contrast, during the El Niño event (2015-2016) the water supply decreased by 20% and the sediment supply by 50%. Finally, the present water discharge of the Mekong River to the sea can be estimated to be 400km^3/yr, ±100km^3/yr and the present sediment supply to the sea can be estimated to be 40 Mt/yr, ±20 Mt/yr, depending on ENSO events.*

Keywords: *Mekong; river discharge; sediment; ENSO; El Niño; La Niña*

1. Introduction

The Mekong River is the second largest river basin (795×103km^2) after the Yangtze River (1.8×106km^2) and the third in terms of water discharge (after the Ganges-Brahmaputra and the Yantgze Rivers) in Southeast Asia. In recent years, reservoir operation and climate change have strongly affected on hydrological regime of the Mekong River Basin. Many studies have analyzed the impact of climate variability on hydrological conditions in the Mekong River basin and the El Niño Southern Oscillation (ENSO) indices were widely used (e.g. [2,4,5]). They showed that the ENSO phases significantly influence precipitation, runoff, water level and sediment load in the Mekong River basin. Piton and Delcroix [2], based on data from 43 consecutive years of in situ measurement (1960-2002) and seven years of satellite monitoring (1996-2002), demonstrated that El Niño phases were associated to a decrease in rainfall in the middle and lower Mekong basin and to a reduction of water discharge at the Chroy Chang Var station (located in Cambodia). The discharge reduction reached 34% during the strong 1997-1998 El Niño. On the other hand, higher discharges were observed during La Niña events [8].

The Mekong River originates from the Tibetan plateau and flows through a narrow deep gorge along with the Salween and Yangtze Rivers that together are known as the "Three Rivers Area". The Mekong River then flows through Myanmar, Laos, Thailand, and Cambodia before it finally drains into the sea creating a large delta in Viet Nam (Figure 1). The Mekong flows in the delta through two main distributaries: the Tien River (generally referred to as the Mekong River, in the delta) in its eastern part, and the Hau River (the "second river" in Vietnamese, also known as Bassac River) in its western part.

The river discharge of the Mekong is mostly controlled by the tropical monsoon climate, which has distinct wet and dry seasons. Mean annual rainfall varies from 1,000mm in Thailand to 3,200mm in Laos. In the Mekong River basin, 85% of water discharge occurs

Corresponding author: Dang Thi Ha
E-mail: leha1645@yahoo.com

during the flood season and 15% occurs in the low flow season. The discharge is the largest from August-September and the smallest in April-May [7].

This paper is based on the recent extensive dataset of hourly water discharges and twice-daily sediment concentrations, from 2009 to 2016 at 2 strategic sites (Can Tho and My Thuan gauging stations-Figure 1), supplied by the Viet Nam Institute of Meteorology, Hydrology and Climate change (IMHEN). The aim of this study is to analyse the influence of climatic variability on water discharge and sediment flux in the Lower Mekong River.

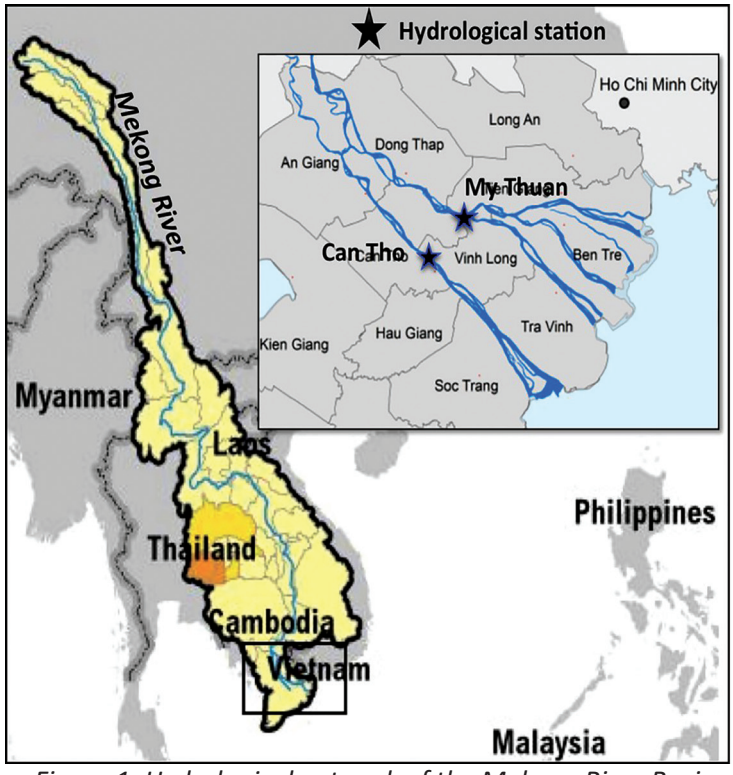

Figure 1. Hydrological network of the Mekong River Basin

2. Data collection and treatment

The sediment flux in ebb tide and flood tide conditions were calculated following:

$Q_{s,e} = Q_e \times C_{av,e}$ and $Q_{s,f} = Q_f \times C_{av,f}$

where Q stands for the water supply during an ebb or flood period, Qs for the suspended sediment supply during this period, Cav for the average suspended sediment concentration, and subscripts e and f stand for ebb and flood, respectively.

The monthly net sediment flux (Qs j, in Mt/month) of month j was then computed from the contributions of all ebb tides and flood tides of the month:

$$Qs_j = \sum_{i=1}^{i=n} Qs._{ei} - \sum_{i=1}^{i=n} Qs._{fi}$$

where n stands for the number of days in month j, and the annual sediment flux (Qs_a, in Mt) from:

$$Qs_a = \sum_{j=1}^{12} Qs_j$$

For the information of climatic variations, in particular to assess the impact of ENSO on the water and sediment supplies, different indexes were considered, provided by the National Oceanic and Atmospheric Administration (NOAA, e.g. Sea Surface Temperature - SST, Southern Oscillation Index - SOI,...) and the Southern Oscillation Index (SOI) was often used [1,2,6]. Prolonged periods of negative SOI values coincide with abnormally warm ocean waters across the eastern tropical Pacific typical of

El Niño episodes, whereas prolonged periods of positive SOI values coincide with abnormally cold ocean waters across the eastern tropical Pacific typical of La Niña episodes. Sustained positive SOI values above about +8 indicate a La Niña event while sustained negative values below about –8 indicate an El Niño.

In this paper, the data of SOI was downloaded from the website https://www.cpc.ncep.noaa.gov/products/precip/CWlink/MJO/enso.shtml [5]). The Figure 2 displays the ENSO events using monthly SOI anomalies. Based on time series of SOI anomaly between 2009 and 2016 in Figure 2, we observed one obvious El Niño event (2010-2011) and one obvious La Niña event (2015-2016).

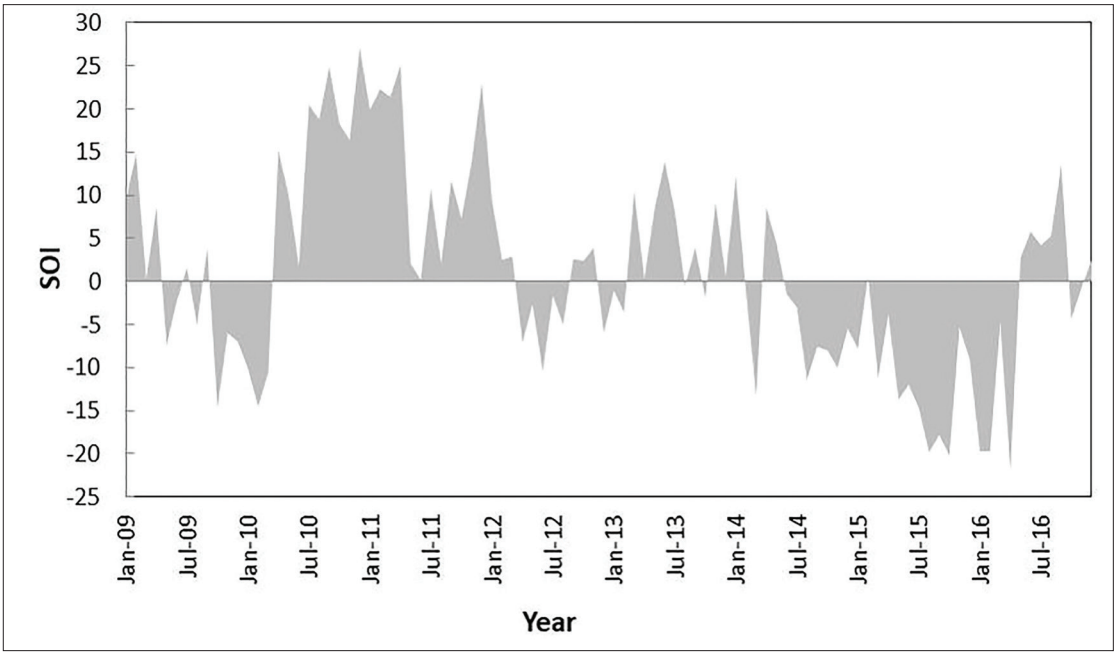

Figure 2. Time series of SOI anomalies. Positive SOI values above about +8 indicate a La Niña event while negative values below about - 8 indicate an El Niño

3. Results and Discussions

3.1. Monthly Averages and Annual Variations of Flux - in and flux Out in the Estuaries

The monthly and yearly values of sediment flux flowing seaward (flux-out) and landward (flux-in) at CanTho and MyThuan stations were calculated over the eight-year monitoring period (2009-2016) and are presented in Figures 2 and 3. We observed that the monthly evolution of sediment flux flowing seaward and landward at both stations experienced strong seasonal variations (Figure 2). At the Can Tho station, the monthly sediment flux-out ranged between 0.14 and 10.5 Mt/month (average value of 1.5 Mt/month) with the highest value observed in rainy season. The highest values of sediment flux-in were observed in dry season with individual values varying from 0.01 to 0.45 Mt/month (average value of 0.16 Mt/month). A similar evolution of sediment flux-in and-out was observed at the My Thuan station (Figure 3).

The trend to a decrease in the yearly flux flowing out (Figure 4) should be analyzed with care, since the study period encompassed an excess of discharge at the beginning of the study period with the La Niña event of 2010-2011, and ended with a deficit of discharge associated to the El Niño event of 2015-2016. The trend is almost nil at Can Tho, while a short increase in landward sediment flux was observed at My Thuan station, showing slight impact by the ENSO variation in My Thuan (Figure 4). The difference in the trends between the two stations may be partly explained by other factors than El Niño, such as sand mining activities [1, 3].

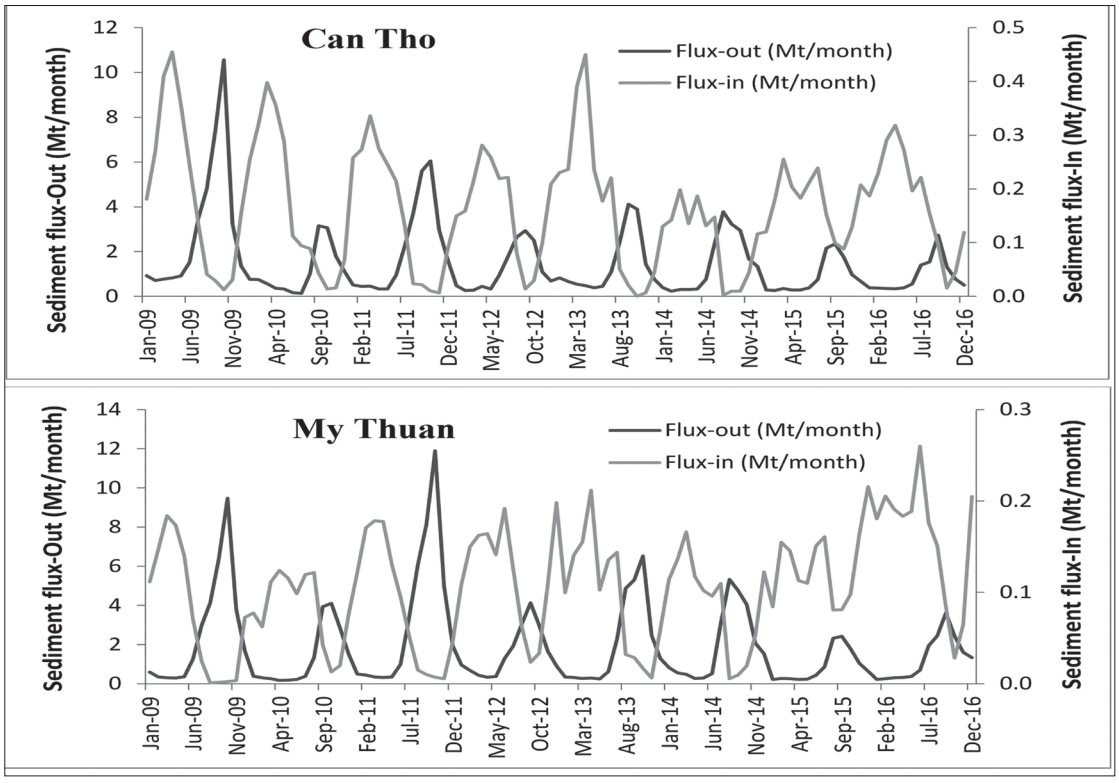

Figure 3. Evolution of monthly sediment fluxes oriented seaward and landward at Can Tho and My Thuan stations for the period 2009-2016

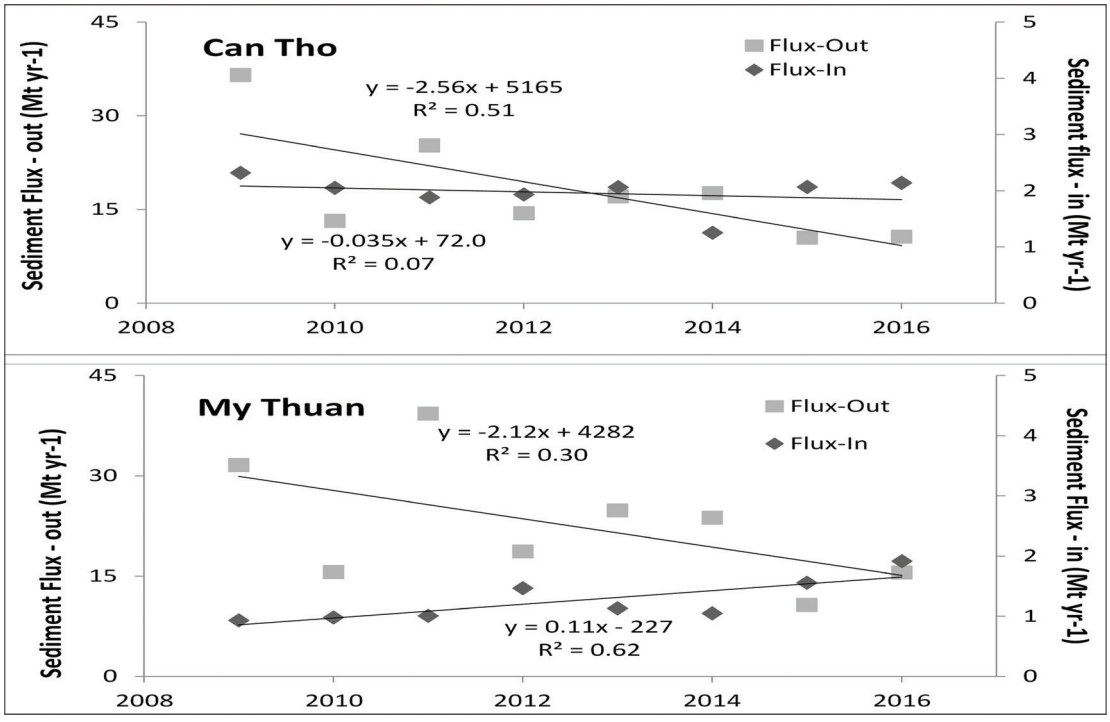

Figure 4. Evolution of annual sediment fluxes oriented seaward and landward at Can Tho and My Thuan stations for the period 2009-2016

3.2 Influences of ENSO on Seasonal and Annual Sediment Supply

In order to assess the influence of ENSO on suspended sediment fluxes at monthly and annual scales, we compared the monthly and yearly values of 2010-2011 (affected by the 2010 La Niña, Figure 2), 2015-2016 (affected by the strong 2015 El Niño, Figure 2), to the ones averaged over 2009 and 2012-2014. The monthly values are presented in Figure 5, and the yearly averaged values, per period, for Q and Qs, are given in Table 1.

The influence of El Niño and La Niña on the monthly and yearly Q and Qs are very clear in comparison with neutral years:

- In 2010-2011 (affected by La Niña of 2010), the flux of water flowing to the sea of the Mekong River (Can Tho + My Thuan) increased by ~22% and the flux of water entering in the estuaries decreased by more than 10%. Globally, the net seaward flux of water increased by 29.6%. The sediment supply by the river increased by ~51% and the sediment flux inland decreased by 15%, providing a net increase of sediment supply to the sea by 55.6%.

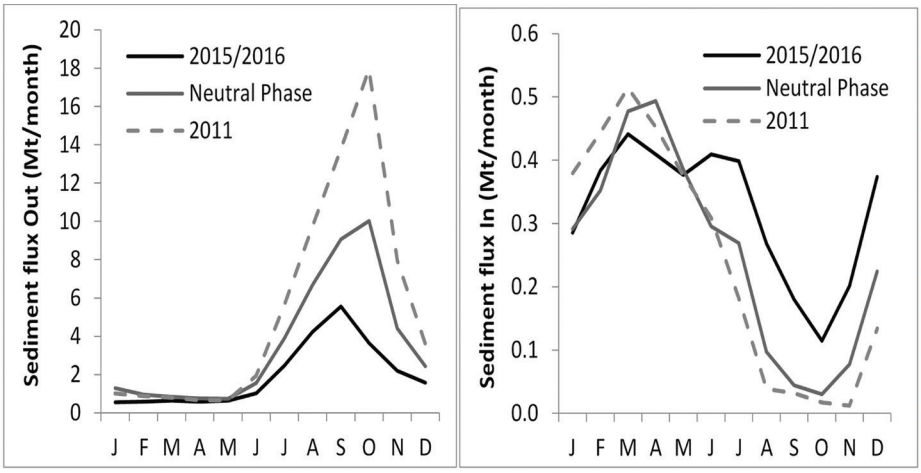

Figure 5. Monthly evolution of the sediment flux-out and flux-in of the Mekong River

Table 1. Average yearly water and sediment discharges at Can Tho and My Thuan stations during different ENSO stages over the 2009-2016 period. (in km³/yr; ** in Mt/yr)*

Period	Can Tho			My Thuan			Can Tho + My Thuan		
	Flux In	Flux Out	Total	Flux In	Flux Out	Total	Flux In	Flux Out	Total
Q 2010-2011 (La Niña)*	47.9	290.2	242.3	36.7	307.9	271.2	84.6	598.1	513.5
Q 2015-16 (El Niño)*	70.7	221.1	150.4	57.1	221.6	164.5	127.8	442.7	314.9
Q 2009,2012-2014 Neutral phase*	54.4	245.2	190.8	40.4	245.6	205.2	94.9	490.9	396.0
Qs 2011 (La Niña)**	1.88	25.25	23.37	1.01	39.33	38.32	2.89	64.58	61.69
Qs 2015-16 (El Niño)**	2.11	10.58	8.47	1.74	13.13	11.39	3.84	23.70	19.86
Qs 2009,2012-2014 neutral phase**	1.93	19.77	17.85	1.11	22.91	21.80	3.04	42.68	39.65

- In 2015-2016 (affected by El Niño of 2015), the flux of water flowing to the sea of the Mekong River (Can Tho + My Thuan) decreased by ~10% and the flux of water entering in the estuaries increased by more than 34%. Globally, the net seaward flux of water decreased by 20.5%. The sediment supply by the river decreased by ~45% and the sediment flux inland increased by 26%, providing a net decrease of sediment supply to the sea by 50%.

The flux back to the estuaries evolves the opposite of the flux seaward. The effect of ENSO on the sediment fluxes (in and out) is mainly sensitive in flood season (Figure 5).

In conclusion, the water flux to the sea was 396km^3/yr, and the sediment supply to the sea was 39.65Mt/yr in average over the neutral years. La Niña was seen to increase the water supply by almost 30% and the sediment supply by 55%. El Niño was seen to decrease the water supply by 20% and the sediment supply by 50%.

4. Conclusions

The benefit of regular measurements at each flood and ebb stages from 2009 to 2016 is to provide, for the first time, an estimate of both sediment fluxes flowing seaward and landward in the estuaries. Our results showed that during 2009-2016 period at both stations measured, the monthly sediment flux flowing seaward was very high in rainy season. In contract, the highest values of monthly sediment flux landward were observed in dry season. The present water discharge of the Mekong River to the sea can be estimated to be 400km^3/yr, ± 100km^3/yr depending on ENSO, and the present sediment supply to the sea can be estimated to be 40Mt/yr, ± 20Mt/yr, depending on ENSO.

In added, we observed that the water discharge and annual sediment supplies by the Mekong strongly influenced by ENSO events. In fact, the water supply increased by almost 29.6% and the sediment supply by 55.6% due to La Niña event of 2010-2011; the water supply decreased by about 20.5% and the sediment supply by 50% due to El Niño event of 2015-2016. However, we noted that the long-term observation (>10 years) is needed in order to deeply analyse the impacts of the climatic change on the hydrological regime in the lower Mekong River.

References

1. Anthony, E.J.; Brunier, G.; Besset, M.; Goichot, M.; Dussouillez, P.; Nguyen, V.L. *Linking rapid erosion of the Mekong River delta to human activities. Sci. Rep. 2015, 5, 14745, doi:10.1038/srep14745*.
2. Kondolf, G.M.; Schmitt, R.J.P.; Carling, P.; Darby, P.; Arias, M.; Bizzi, S.; Castelletti, A.; Cochrane, T.A.; Gibson, S.; Kummu, M.; et al. *Changing sediment budget of the Mekong: Cumulative threats and management strategies for a large river basin. Sci. Total Environ. 2018, 625, 114-134, doi:10.1016/j. scitotenv.2017.11.361.*
3. Ogston, A.S.; Allison, M.A.; McLachlan, R.L.; Nowacki, D.J.; Stephens, J.D. *How tidal processes impact the transfer of sediment from source to sink: Mekong River collaborative studies. Oceanography 2017, 30, 22–33, doi:10.5670/oceanog.2017.311.*
4. Piton, V.; Delcroix, T. *Seasonal and interannual (ENSO) climate variabilities and trends in the South China Sea over the last three decades. Ocean Sci. Discuss. 2018, doi:10.5194/os-2017-104.*
5. Sea Surface Temperature (SST). *Available online: https://www.cpc.ncep.noaa.gov/products/ precip/CWlink/MJO/enso.shtml / (accessed on 20 December 2017).*
6. Wang, H.; Saito, Y.; Zhang, Y.; Bi, N.; Sun, X.; Yang, Z. *Recent changes of sediment flux to the western Pacific Ocean from major rivers in East and Southeast Asia. Earth-Sci. Rev. 2011, 108, 80–100, doi:10.1016/j.earscirev.2011.06.003.*
7. Wang, J.J.; Lu, X.X.; Kummu, M. *Sediment load estimates and variations in the lower Mekong River. River Res. Appl. 2011, 27, 33-46, doi:10.1002/rra.1337.*
8. Xue, Z.; Liu, J.P.; Ge, Q.A. *Changes in hydrology and sediment delivery of the Mekong River in the last 50 years: Connection to damming, monsoon, and ENSO. Earth Surf. Proc. Land. 2011, 36, 296–308, doi:10.1002/esp.2036.*

FLOODING IMPACTS ON RICE CULTIVATING AREA UNDER CLIMATE CHANGE IN TRA VINH PROVINCE

Mai Van Khiem[(1)], Tran Tuan Hoang[(1)], Phan Thi Diem Quy[(1)]
Huynh Thi My Linh[(1)], Ho Cong Toan [(1)], Pham Thanh Long[(1)], Nguyen Thi Thu Hang[(2)]
[(1)]Viet Nam Institute of Meteorology, Hydrology and Climate Change
[(2)]Sai Gon University

Received: 7 January 2019; Accepted: 11 February 2019

Abstract: *Climate change (CC) and sea level rise (SLR) are a challenge for many ecosystems, biodiversity and environmental resources, greatly influencing human social life. In this paper, we assess the impact of flooding in the rice cultivating area under climate change and sea level rise by 2100 in Tra Vinh province, through gathering and inheriting database methods, model (MIKE FLOOD) and geographic information system. The results indicated that Cau Ke and Chau Thanh districts have flooded areas on rice growing land larger than other districts. The results obtained in this study can be used to provide options for crop improvement, food security in the region and contributing to the local sustainable development.*

Keywords: *Climate change, sea level rise, rice cultivation area, Tra Vinh, MIKE FLOOD*

1. Introduction

Rice cultivation in Viet Nam was closely associated with the rural population and traditional farmers. Long-term flooding greatly affects cultivated land, rice production, affecting the food security of the province in particular and the Mekong Delta region in general. Under the scenario of climate change and sea level rise for Vietnam to be built and announced in 2016, about 38.9% of the Mekong Delta area will be at risk of flooding if sea level rises by 100cm. Tra Vinh province alone will have a risk of flooding of 21.3% compared to the natural area of the province [1].

Tra Vinh is adjacent to Ben Tre, Vinh Long and Soc Trang provinces; located between Tien River and Hau River (Figure 1). Tra Vinh provincial centre is 130km from Ho Chi Minh City and 100 km from Can Tho city. Tra Vinh province has 1 city, 1 town and 07 districts. Natural land area of Tra Vinh is 235,826ha [2]. Every year, the rice cultivation area of Tra Vinh is quite large. According to Tra Vinh Statistical Office, the total area of 2016 rice cultivation is 234,247ha [6].

Corresponding author: Pham Thanh Long
E-mail: longpham.sihymete@gmail.com

The advantage of the province is wet rice agriculture, the annual area of rice cultivation in Tra Vinh province faces many problems of natural disasters such as drought, saline intrusion, especially inundation. Flooding causes much damage to rice as well as damaging crops, reducing rice productivity. In addition, flooding also causes epidemics to reduce both yield and quality of rice.

In the context of climate change that is increasingly harsh and unpredictable, studies of sea level rise causing flooding on rice are essential.

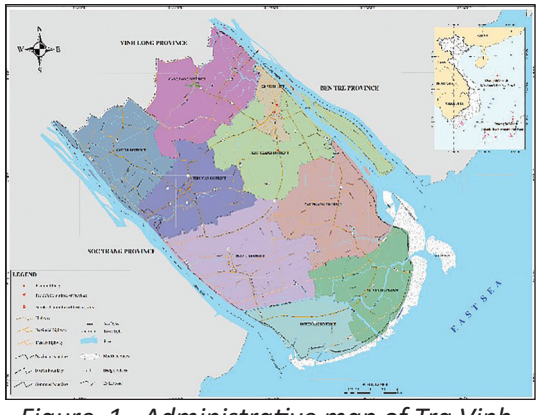

Figure 1. Administrative map of Tra Vinh province

2. Methodology

(1). Methods of gathering and inheriting databases

This method is implemented on the basis of inheriting, analysing, and synthesizing relevant sources of documents, materials, and data in a selective way. After that, assessed according to the requirements and purpose of the study. In this study, the gathered and inherited sources of documents and data include: flow and water level data provided by the Southern Regional Hydrometeorological Center; Hydraulic diagram and river section are measured and collected from research projects and projects directly implemented by the Sub-Institute of Hydro Meteorology and Climate Change.

(2). Model method

The modelling method is widely used in flood simulation and mapping. In particular, the one-way hydraulic model combines GIS such as MIKE 11, ISIS, VRSAP, HydroGIS, integrated 1-way and 2-way or 2-way (full 2D) models such as MIKE FLOOD (MIKE 21 and MIKE 11 integration), MIKE 21, SOLBECK, TELEMAC [3]. In this article, MIKE FLOOD model was used in linking MIKE 11 HD and MIKE 21 FM modules.

MIKE 11 model is a one-way hydraulic model, in which the hydrodynamic module is a central part, simulating the dynamic process along the unstable flow length with the combination of equation continuous and momentum equations (Saint-Venant equations):

The continuity equation [4]:

$$B\frac{\partial h}{\partial t}+\frac{\partial Q}{\partial x}=q$$

The momentum equation [5]:

$$\frac{\partial Q}{\partial t}+\frac{\partial}{\partial x}\left(\alpha\frac{Q^2}{A}\right)+gA\frac{\partial h}{\partial x}+g\frac{Q|Q|}{AC^2R}=0$$

MIKE 21 FM model includes:

The continuity equation [5]:

$$\frac{\partial h}{\partial t}+\frac{\partial hu}{\partial x}+\frac{\partial hv}{\partial y}=hS$$

The shallow water equation [6]:

$$\frac{\partial h\bar{u}}{\partial t}+\frac{\partial hu^2}{\partial x}+\frac{\partial h\overline{uv}}{\partial y}=f\bar{v}h-gh\frac{\partial \eta}{\partial x}-\frac{h}{\rho_0}\frac{\partial p_a}{\partial x}-\frac{gh^2}{2\rho_0}\frac{\partial \rho}{\partial x}+$$

$$\frac{\tau_{sx}}{\rho_0}-\frac{\tau_{bx}}{\rho_0}-\frac{1}{\rho_0}\left(\frac{\partial S_{xx}}{\partial x}+\frac{\partial S_{xy}}{\partial y}\right)+\frac{\partial}{\partial x}\left(hT_{xx}\right)+\frac{\partial}{\partial y}\left(hT_{xy}\right)+hu_sS$$

$$\frac{\partial h\bar{v}}{\partial t}+\frac{\partial h\overline{uv}}{\partial x}+\frac{\partial h\overline{v^2}}{\partial y}=-f\bar{u}h-gh\frac{\partial \eta}{\partial y}-\frac{h}{\rho_0}\frac{\partial p_a}{\partial y}-\frac{gh^2}{2\rho_0}\frac{\partial \rho}{\partial y}+$$

$$\frac{\tau_{sy}}{\rho_0}-\frac{\tau_{by}}{\rho_0}-\frac{1}{\rho_0}\left(\frac{\partial S_{yx}}{\partial x}+\frac{\partial S_{yy}}{\partial y}\right)+\frac{\partial}{\partial x}\left(hT_{xy}\right)+\frac{\partial}{\partial y}\left(hT_{yy}\right)+hv_sS$$

(3) GIS method

Map tools such as Mapinfo and ArcGIS are used to extract the results of the model, serve the management and exploitation of information and overlap to build flood risk maps.

3. Input data for models

Based on data from the river network throughout the lower Mekong Delta River (see Figure 2) in the project "Update climate change scenarios in Tra Vinh province under the 2016 scenario according to the Ministry of Natural Resources and Environment" , we used to calibrate and validate hydraulic models for Tra Vinh province. After achieving the good results, we extracted separate river, cross-sections and boundary data for Tra Vinh province (see Figure 3).

Model input data for river network in Mekong Delta River, include:

- Documents on the design of irrigation works, irrigation systems in the lower Mekong area of the Southern Institute of Water Resources Research from 2002 to the present and have been provided by Departments of Tra Vinh province.

- Boundary conditions: water level and discharge in 2016 were collected from Southern Regional HydroMeteorology Center

- Climate change and sea level rise scenarios have been used in this study was the set of "Climate change and sea level rise scenarios for Vietnam" newest update of 2016 of Ministry of Natural Resources and Environment.

- Hydraulic diagram of river network in Mekong Delta River including: main rivers and canals such as Tien river, Hau river, Vam Nao river, Co Chien river and other small river branches have been set up based on satellite maps and hydrological maps of the Mekong Delta River region with 1,116 branches. The

number of points calculated in the model were about 13,000 points. River sections: about more than 5,000 sections across the Mekong Delta river system.

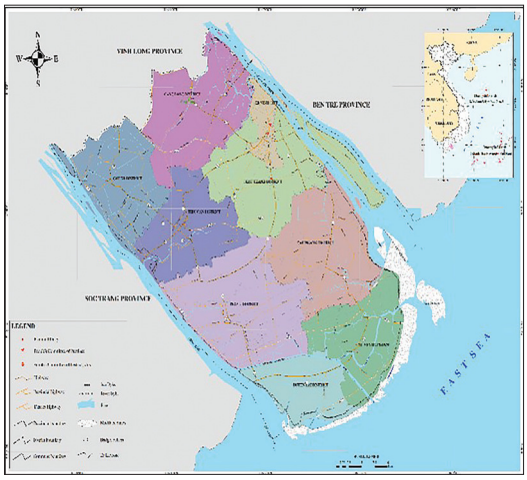

Figure 2. Hydrodynamic diagram of river network in Mekong Delta River

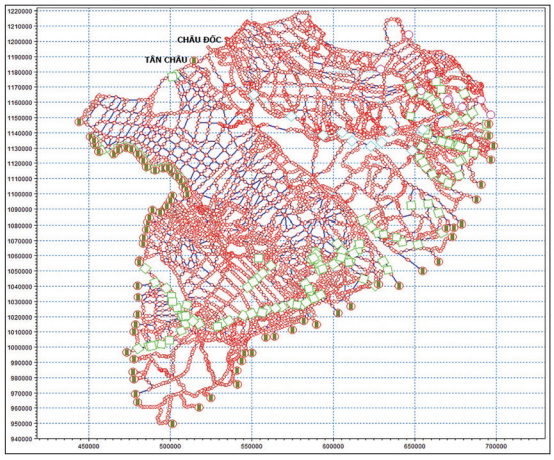

Figure 3. The river network uses flood calculation for Tra Vinh province

- Hydraulic modules are built based on 2 main flow profiles in Tan Chau and Chau Doc in 2016. Other discharge margins without other rivers or small canals starting in the field are priced value of 0 m3/s. There for, hydraulic diagram including real measured datas in Tan Chau and Chau Doc Stations in 2016.

- Data of water level in coastal estuaries is taken as downstream boundary used in the model is the actual data measured in 2016 at coastal stations such as Vam Kenh station (Tieu gate), Binh Dai station (Dai gate), An Thuan (Ham Luong gate), Ben Trai (Co Chien gate), and My Thanh station (My Thanh, Dinh An gates) and Tran De station (Tran De gate).

- The system of checking water level data includes data at hydrological stations such as Vam Nao, My Thuan, My Tho (Tien river), Can Tho, Dai Ngai, Tran De (Hau river) or Cho Lach station, Tra Vinh (Co Chien river) and My Hoa (Ham Luong river) are collected at the Hydrological Meteorological Station in the Southern region in 2016, serving for model calibration and validation. This set of data ensures reliability and accuracy for model calculation and correction.

Input data for river network is calculated for Tra Vinh province:

- The boundaries have been used in the river network of Tra Vinh province include the upper boundary which is the data of water level and flow extracted from the Mekong Delta River network (downscaling), including the boundary of Can Tho, My Thuan (water level data and flow data). Downstream boundaries were downstream water level in 2016 at hydrological stations such as Ben Trai station and Tran De station. Figure 3 shows the river network of Tra Vinh province extracted from river network of Mekong Delta River region.

- Topography has been used in flood calculation for Tra Vinh province was Digital Elevation Models (DEM) topography data of Viet Nam Ministry of Natural Resources and Environment (MONRE), with dimensions of 10x10 meter (see Figure 4).

- Topographic data have been used to construct the topography and calculate for the MIKE FLOOD model and the MIKE 21FM model, as follows: topographic data has been extracted from 1: 200,000 map of the Vietnamese People's Navy, published in 2009; in addition, the study area topography has been also measured during the 2016 survey in the project "Climate Change Adaptation in the Mekong Delta in Tra Vinh Province (Tra Vinh AMD Project)". It included 78,489 elements and 39,678 nodes (see Figure 5)

- River network in MIKE 11HD model was linked to topography of MIKE 21FM in MIKE FLOOD model by lateral link (see Figure 6).

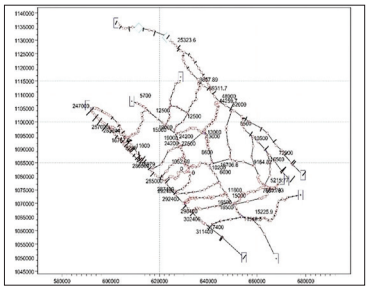

Figue 4. DEM topography data for Tra Vinh province

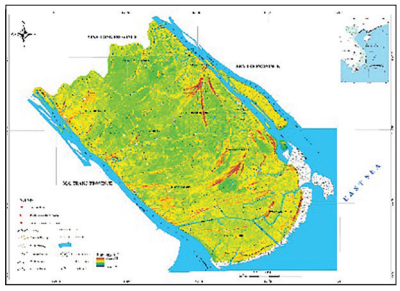

Figue 5. Topography data in MIKE 21FM model

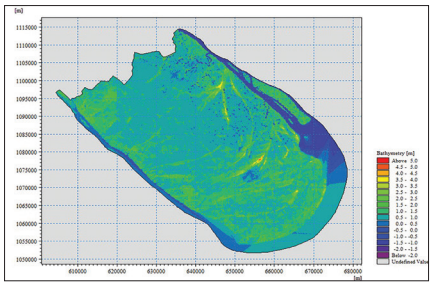

Figue 6. Lateral link between MIKE 11HD model and MIKE 21FM model

4. Results

4.1. Calibration and validation of models

The hydraulic model of saline intrusion calculation has been calibrated, validated based on the actual measured data at Tra Vinh station in 2016 and 2010. Data were collected from Southern Regional HydroMeteorology Center. Stations location is shown in the Figure 7.

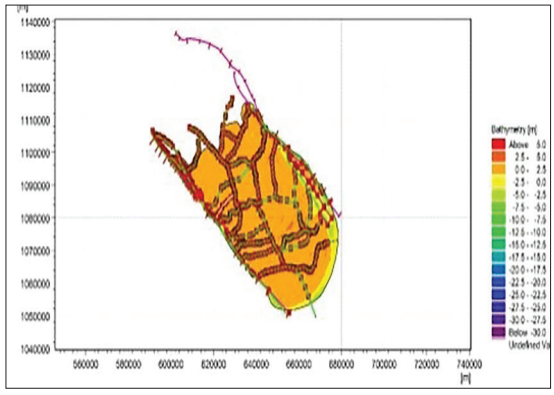

Figure 7. Location map of hydrological stations in Southern of Viet Nam

- Manning roughness coefficient has been adjusted from 30 to 65 depending on the river section;

- Initial conditions: The water level was 0.5m and the flow was equal to 5m^3/s for the entire river system;

- Time step for hydraulic calculation (HD) Δt = 5 minutes.

- Time to calibrate model parameters from July 1, 2016 to July 31, 2016 and validate in the period of July 1, 2010 to July 31, 2010. The results of the water level calculation in the above time were compared with the actual measured data based on the correlation coefficient and the NASH suitability index and the hydraulic model calibration results are shown below.

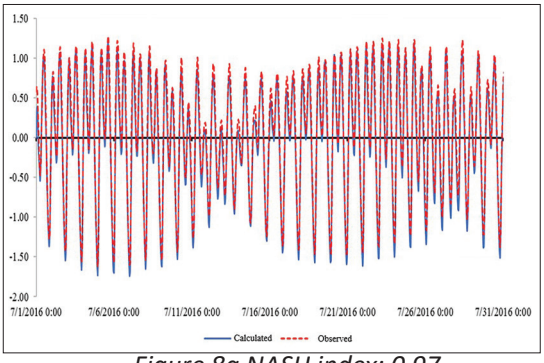

Figure 8a NASH index: 0.97

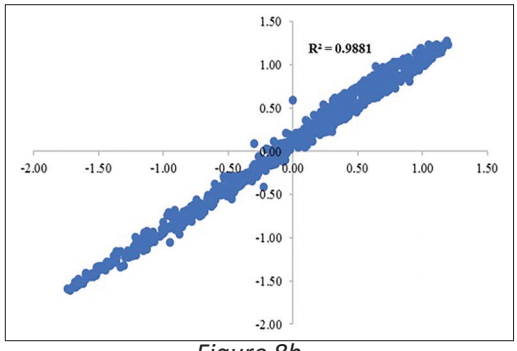

Figure 8b

Figure 8 (a-b): Calibration water level at Tra Vinh Station in July 2016

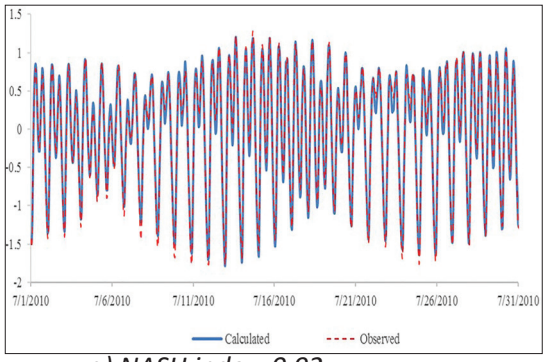

a) NASH index: 0.92

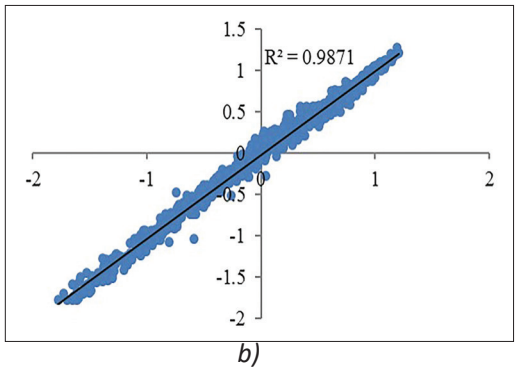

b)

Figure 9 (a-b). Validation water level at Tra Vinh Station in July 2010

Calculation results and actual measured data of water level satisfying the permissible error limit of value and tidal phase for the NASH coefficient in the range of 0.92-0.97. Thus, the data set used to build the model and the model correction parameter set were reliable.

4.2. Simulation results and updated maps flooded on rice cultivation land for Tra Vinh province

We carried out the calculation and comparison of flooding levels on rice cultivation land in 2016 in the current situation (in 2016) and climate change scenarios (2025, 2050, 2070, 2100). According to the land use planning map, the area of land for rice cultivation in Tra Vinh in 2016 was about 99,822.47 hectares.

(1). Current status of flooding in 2016

The flooded map of Tra Vinh province according to the current status 2016 is presented in Figure 10.

The total flooded area was 23,497.68 ha, accounting for nearly 10% of the province's natural land area. The total area of flooded rice paddy land was 4,211.11 hectares, accounting for about 4.2% of the province's paddy land.

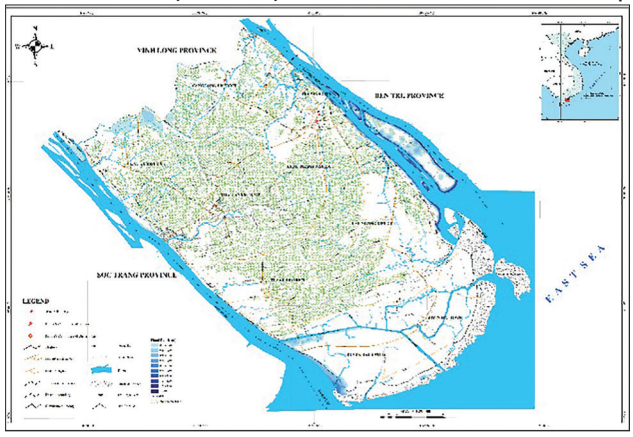

Figure 10. Map flooded in Tra Vinh province in 2016

(2). Forecasting the risk of flooding on rice cultivation land until 2025

To simulated and updated the flood risk map on rice cultivation land in Tra Vinh province until 2025, the study used Sea level rise for Vietnam was published by the Ministry of Natural Resources and Environment in 2016. Accordingly, in 2025, sea level rise will be 0.12m for RCP4.5 [1]. Flood hazard map of Tra Vinh rice land in 2025 is shown in Figure 11.

The total flooded area will be 26,491 hectares, accounting for about 11.2% of the province's natural land area.

The total area of flooded rice paddy land will be 5,531.7 hectares, accounting for about 5.5% of the province's rice cultivation land.

Figure 11. Flood risk map according to scenario RCP4.5_2025 and current status of wet rice cultivation in Tra Vinh province

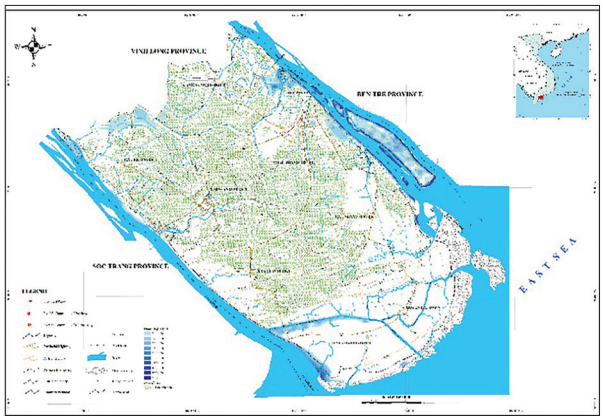

Figure 12. Flood risk map according to scenario RCP4.5_2050 and current status of wet rice cultivation in Tra Vinh province

(3) Forecasting the risk of flooding on rice cultivation land until 2050

To simulated and update the flood hazard map on the rice cultivation land in Tra Vinh province until 2050, the study used Sea level rise for Viet Nam was published by the Ministry of Natural Resources and Environment in 2016. Accordingly, in 2050, sea level rise will be 0.22 m corresponding to RCP4.5 [1]. The risk map of flooding in Tra Vinh rice land in 2050 is shown in Figure 12. The total flooded area will be about 28,762 hectares, accounting for 12.2% of the natural land area. The total area of flooded rice paddy land will be 6,815 hectares, accounting for 6.8% of the province's rice cultivation land area.

(4) Forecasting the risk of flooding on rice cultivation land until 2070

To simulated and updated the flood hazard map on the paddy land in Tra Vinh province until 2070, the study used Sea level rise for Viet Nam was published by the Ministry of Natural Resources and Environment in 2016. Accordingly, in 2025, sea level rise will be 0.33 m for RCP4.5 [1]. Flood hazard map of Tra Vinh paddy land in 2070 is shown in Figure 13.

The total flooded area will be 32,101 hectares, accounting for 13.6% of the natural land area. The total flooded area on paddy land will be 8,231 hectares, accounting for 8.2% of the province's rice land.

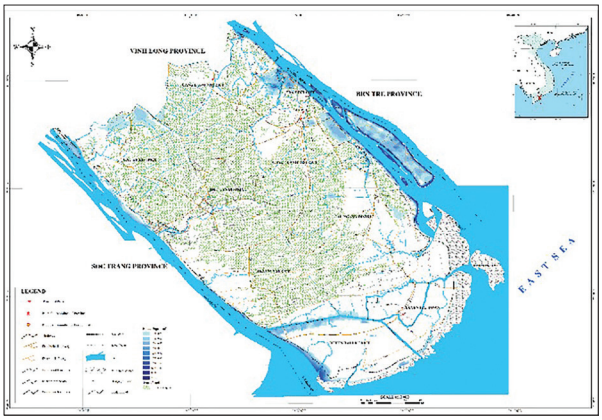

Figure 13. Flood risk map according to RCP4.5_2070 scenario and current status of wet rice cultivation in Tra Vinh province

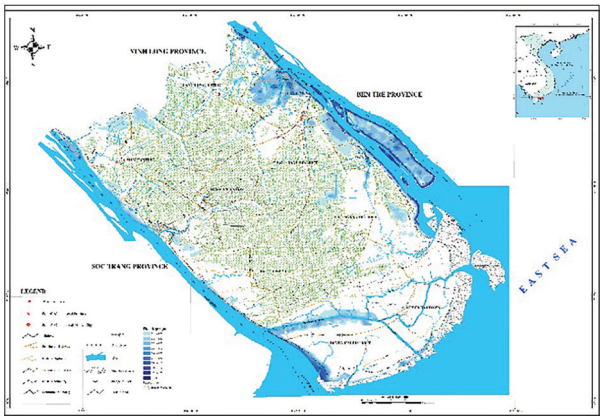

Figure 14. Flood risk map according to RCP4.5_2100 scenario and current status of wet rice cultivation in Tra Vinh province

(5). Forecasting the risk of flooding on rice cultivation land until 2100

To simulated and updated the flood hazard map on the paddy land in Tra Vinh province until 2100, the study used Sea level rise for Viet Nam was published by the Ministry of Natural Resources and Environment in 2016. Accordingly, in 2025, Sea level rise will be 0.53m for RCP4.5 [1]. The flood risk map of Tra Vinh rice land in 2100 is shown in Figure 14.

The total flooded area will be 41,159 hectares, accounting for 17.5% of the natural land area. The total area of flooded rice paddy land will be 12,214 hectares, accounting for 12.2% of the province's rice growing area.

Statistics of the current flooded area in 2016 and the RCP4.5 scenarios in 2025, 2030, 2050, 2100 on the area of rice cultivation and the increase/decrease compared to 2016 is presented in tables 1, 2 , 3, 4 below.

Table 1. Statistics of flooded areas in Tra Vinh province over the years

Number	Flooding level (m)	Flooded area (hectares)				
		2016	45_2025	45_2050	45_2070	45_2100
1	0.1-0.2	5,830.61	6,729.02	6,803.48	7,259.09	9,015.82
2	0.2-0.3	2,803.63	3,773.24	4,681.73	4,975.96	6,137.65
3	0.3-0.5	3,026.27	3,482.81	4,127.96	5,482.37	9,070.76
4	0.5-0.6	1301.59	1,301.92	1,254.12	1,367.75	2,132.33
5	0.6-0.7	1,117.84	1,226.62	1,296.25	1,211.78	1,505.16
6	0.7-0.8	1,021.75	1,056.04	1,139.55	1,264.21	1,225.00
7	0.8-1.0	1,390.22	1,632.85	1,822.34	2,048.54	2,331.98
8	1.0-1.2	1,074.83	1,143.94	1,213.14	1,377.83	1,766.99
9	1.2-1.5	1,232.46	1,267.89	1,311.44	1,427.26	1,699.25
10	>1.5	4,698.48	4,876.45	5,112.14	5,686.92	6,274.26
	Total	**23,497.68**	**26,490.77**	**28,762.16**	**32,101.71**	**41,159.21**

Table 2. Statistics difference in flooded area according to the schedule compared to the area flooded in Tra Vinh province in 2016

Number	Flooding level (m)	Flooded area compared to 2016 (hectares)			
		45_2025	45_2050	45_2070	45_2100
1	0.1-0.2	+898.40	+972.87	+1,428.48	+3,185.21
2	0.2-0.3	+969.60	+1,878.09	+2,172.33	+3,334.02
3	0.3-0.5	+456.54	+1,101.69	+2,456.10	+6,044.49
4	0.5-0.6	+0.33	-47.47	+66.15	+830.73
5	0.6-0.7	+108.78	+178.41	+93.94	+387.33
6	0.7-0.8	+34.29	+117.80	+242.46	+203.25
7	0.8-1.0	+242.63	+432.13	+658.32	+941.76
8	1.0-1.2	+69.11	+138.31	+303	+692.16
9	1.2-1.5	+35.43	+78.98	+194.80	+466.79
10	>1.5	+177.97	+413.66	+988.44	+1,575.78
	Total	**+2,993.09**	**+5,264.47**	**+8,604.03**	**+17,661.53**

(+: increase: -: decrease)

Table 3. Statistics of flooded areas on rice cultivation land in Tra Vinh province over the years

Number	Flooding level (m)	The area is flooded on the current land for rice cultivation (hectares)				
		2016	45_2025	45_2050	45_2070	45_2100
1	0.1-0.2	2,040.85	2,806.62	2,944.22	3,011.01	4,241.34
2	0.2-0.3	702.57	1,000.42	1,655.20	2,072.49	2,388.25
3	0.3-0.5	371.57	549.81	843.70	1,482.12	3,231.44
4	0.5-0.6	85.29	119.63	184.53	283.93	557.52
5	0.6-0.7	71.95	73.48	103.20	157.96	342.48
6	0.7-0.8	81.14	68.67	69.03	92.51	192.40
7	0.8-1.0	193.55	172.77	164.71	155.99	197.81
8	1.0-1.2	145.87	174.30	198.20	205.19	161.89
9	1.2-1.5	159.21	165.34	183.50	227.34	280.48
10	>1.5	359.10	400.66	468.84	542.76	620.50
	Total	**4,211.11**	**5,531.70**	**6,815.11**	**8,231.28**	**12,214.12**

Table 4. Statistics of the difference of flooded area on rice cultivation land according to the schedule compared to the area flooded in Tra Vinh province in 2016

Number	Flooding level (m)	Difference in area flooded on rice cultivation land compared to 2016 (hectares)			
		45_2025	45_2050	45_2070	45_2100
1	0.1-0.2	+765.77	+903.37	+970.16	+2,200.49
2	0.2-0.3	+297.85	+952.63	+1,369.91	+1,685.67
3	0.3-0.5	+178.24	+472.13	+1,110.55	+2,859.87
4	0.5-0.6	+34.34	+99.23	+198.63	+472.23
5	0.6-0.7	+1.53	+31.25	+86.00	+270.53
6	0.7-0.8	-12.47	-12.11	+11.37	+111.26
7	0.8-1.0	-20.78	-28.84	-37.56	+4.26
8	1.0-1.2	+28.43	+52.32	+59.32	+16.02
9	1.2-1.5	+6.12	+24.29	+68.12	+121.27
10	>1.5	41.55	+109.73	+183.65	+261.40
	Total	**+1,320.59**	**+2,604.00**	**+4,020.17**	**+8,003.00**

(+: increase: -: decrease)

According to the flooded statistics on the natural land of Tra Vinh province, the current situation and climate change scenarios, the total flooded area on natural land gradually increases over the years. In which the total flooded area of the scenario RCP45_2100 is the largest of 41,159.21 hectares, an increase of 17,661.53 hectares compared to the current situation in 2016. The common flood level is from 0.1-0.2 m for the current situation in 2016, the scenarios RCP45_2025, RCP45_2050, RCP45_2070. For RCP45_2100 scenario, the common flood level is from 0.3 to 0.5 m.

The total flooded area on rice cultivation land also tends to increase, the total flooded area on the rice paddy scenario RCP45_2100 is the largest of 12,214.12 hectares, an increase of 8.003 hectares compared to the current

situation in 2016. In particular, the common flood level on the paddy land from 0.1-0.2m for all years.

5. Concluding

This study has applied the model MIKE FLOOD to simulate the risk of flooding on rice cultivation land in Tra Vinh province according to the 2016 status and the average emission scenarios (RCP4.5) in 2025, 2050, 2070, 2100. From the calculation results, the study has constructed flooded maps on rice cultivation land for Tra Vinh province.

The simulation results, overlapping map and calculating the risk of flooding on rice cultivation land for Tra Vinh province shows: The risk of flooding in 2025 will be about 5,531.7 hectares, accounting for 5.5% of the province's rice cultivation land area; For 2050 will be about 6,815 ha, accounting for 6.8% of the province's rice cultivation land area; For 2070, about 8,231 ha, accounting for 8.2% of the province's rice cultivation land area and in 2100, the risk of flooding will be about 12,214 hectares, accounting for 12.2% of the province's rice cultivation land area. The universal flood level is from 0.1-0.2m, the flood level greater than 1.5m accounts for mainly in the alluvial and canal alluvial areas. According to flooding map then Chau Thanh and Cau Ke districts are the two areas with flooded largest area on rice cultivation land in Tra Vinh province.

Flooding levels in rice and inundation rates are not high, but they also have a certain effect on the yield and quality of local rice. Flooding can cause root rot, reducing yield. Flooding also causes disease to lower the quality of rice. In addition, flooding due to sea level rise also leads to saline intrusion, narrowing the area of land where rice can be cultivated, greatly affecting production and improving fields due to salinity.

At the same time, Tra Vinh province has the sixth rice output in Mekong Delta River region, contributing to ensuring food security in region. Fluctuations in the and yield and quality of rice in the province will significantly affect the region in particular and Viet Nam country in general.

The updated results of the study are the basis for the agencies and agencies in the province to consider and update flood risks due to climate change, sea level rise ink affecting rice land. Since then they have adjusted, integrated climate change issues, sea level rise to future development programs and plans for the province's wet rice, as well as coordinated with neighbouring provinces in the Mekong Delta River region.

The paper only calculated the impact of flooding in the rice growing area, not yet assessed the effect of each flood level, the time to maintain flooding of rice.

References

1. Ministry of Natural Resources and Environment (2016), *Climate Change and Sea level rise scenarios for Viet Nam*, Ha Noi.
2. Tra Vinh Statistical Office (2017), *2016 Statistical Yearbook*, Tra Vinh.
3. Nguyen Hong Quan (2013), "Some methods to build flooded maps of Long An province in conditions of climate change and sea level rise, *Journal of Science and Technology Development,* Vol 16, No. M1-2013, page 32-39.
4. DHI Water & Environment (2017), *MIKE 11 - A Modelling system for Rivers and Channels Reference Manual.*
5. DHI Water & Environment (2017), *MIKE 21 - Flow model FM*.
6. Department of Agriculture and Rural Development in Tra Vinh province, *2016 summarized report and tasks of 2017 plan of Tra Vinh province.*

CALCULATION OF DESIGNED FLOOD IN WEAK DATA REGION IN VIET NAM USING WIN-TR55 MODEL

Doan Thi Noi[(1)], Dang Quang Thinh[(2)]
[(1)]Faculty of Civil Engineering, University of Transport and Communications
[(2)]Institute of Meteorology, Hydrology and Climate Change

Received: 11 February 2019; Accepted: 28 February 2019

Abstract: *Road transportation infrastructure is of great importance in the development of a nation. Viet Nam is facing many challenges in developing road infrastructure due to lack of rainfall and flow data required for calculation of designed flood, especially in mountainous areas. Furthermore, many water drainages have been damaged by heavy rain and severely affected by climate change. In this study, the Win-TR55 based on SCS method is employed for calculating storm runoff volume, discharge and hydrograph to estimate designed flood values for small watersheds. In order to use TR55, parameters for calculating designed flood including rainfall, soil type and land use map are required. This program is widely used in many countries, but has not been applied to the small basins in Viet Nam because of data missing. Tong Soong bridge on the National Highway No.31 crossing Dinh Lap district, Lang Son province, Viet Nam was selected as a case study. The study shows a great potential of the Win-TR55 method to estimate the hydrograph for small and medium watershed in Viet Nam.*

Keywords: *Win-TR55, designed flood, data missing, Tong Soong watershed.*

1. Introduction

Determination of design hydrograph is the key information for construction of transportation infrastructure. The size of these infrastructure systems strongly depends on the design hydrograph to make sure they will not be inundated by flood water in the future. There have been many methods developed to construct the hydrograph [1-2]. In general, these methods construct the designed hydrograph from the designed hyetograph based on the rainfall-runoff relationship. They can be classified into three groups. The first method so-called traditional method uses simple equations to formulate the rainfall-runoff relationship (e.g., runoff coefficient). The advantage of this method is that they can provide quick estimate of designed hydrograph. However, they do not explicitly account for the impact of watershed characteristics such as land use, topography and soil type or watershed conditions such as soil moisture. The second group of methods is based on physically-based hydrological models. These models can well simulate the water dynamics on the watershed but require those data that may be not available in remote regions. The third group of methods uses the conceptual hydrological models.These methods provide relatively accurate estimation of river flow from rainfall with affordable requirement of input data. In these methods, parameters of models are usually estimated from the watershed characteristics using GIS tools. For its accuracy and convenience to estimate, this study uses one of the methods in the third group known as TR55.

In Viet Nam, many studies have been done to develop unit hydrographs. For

Corresponding author: Doan Thi Noi
E-mail: chungnoicg@gmail.com

example, Le Dinh Thanh estimates the portable maximum flood (PMF) from the portable maximum precipitation [4]. Le Van Nghinh documented and applied different methods to calculate designed hyetographs and hydrograph [3]. Ngo Le Long considered the impact of climate change on the estimation of design hydrograph [5]. However, so far there have not been many studies on development of designed hydrograph for small watersheds where the time of concentration is usually less than 10 hours. In these watersheds, using daily rainfall to construct the hydrograph is not suitable due to coarse temporal resolution. Meanwhile, these small watersheds account for up to 70% of drainage structures. In that context, development of designed hydrographs for small watershed is an urgent need.

This study aims at applying the TR55 model based on SCS method to estimate the designed hydrograph for Tong Soong watershed, which is a small mountainous basin in Lang Son province, Northern Viet Nam. In this method, the SCS curve number is employed to estimate runoff and the SCS unit hydrograph is used to estimate the coordinates of hydrograph from runoff.

2. Methodology

This study employed the TR55 software to calculate design hydrographs for small drainage system for Tong Soong watershed. The software was developed in 1998 by the United States Department of Agriculture (USDA, 1999). The TR55 presents simplified procedures for estimating runoff and peak discharges in small watersheds. The model described in TR-55 begins with a rainfall amount uniformly imposed on the watershed over a specified time distribution. Mass rainfall is converted to mass runoff by using a runoff curve number (CN). Runoff is then transformed into a hydrograph by using unit hydrograph theory and routing procedures that depend on runoff travel time through segments of the watershed (USDA, 1999). The software calculates storm runoff volume using the SCS method and constructs hydrograph using tabular hydrograph method. The SCS method estimated by equation below:

$$Q = \frac{(P - 0.2S)^2}{P + 0.8S}$$

where Q is the runoff; P is the rainfall; S is the potential maximum retention after runoff begin. S is related to the soil texture and land cover conditions of the watershed through curve number (CN) parameter by:

$$S = \frac{100}{CN} - 10$$

CN can be determined from soil type, plant cover type, treatment, impervious areas, interception, hydrologic condition and antecedent runoff condition. CN also depends on whether impervious area is directly connected to the drainage system or whether flow over the previous area before reaching the drainage system.

Next, the hydrograph can be constructed for the watershed using tabular hydrograph method as below:

1) Divide the watershed into subareas with relatively homogeneous watershed characteristics

2) The hydrograph coordinate at time t of a subarea (q) is calculated by:

$$q = q_t A_m Q$$

in which q_t is the tabular unit discharge, which is determined from time of concentration (T_c) and ratio between initial abstraction and rainfall (Ia/P) with $I_a = 0.2S$; A_m is the drainage area of subarea; and Q is the runoff on the subarea.

3) Finally, hydrograph at the outlet of the watershed is obtained from the hydrograph coordinates of subareas and time of travel from each subarea to the watershed outlet.

Clearly, there are three main parameters in the TR55 software including CN, Tc and Tt. In this study, these parameters were estimated from maps of topography, land use and soil type.

3. Study area

In this study, we constructed the design hydrograph for the Tong Soong watershed, which is a small watershed in Lang Son province, Northern Viet Nam (Figure 1). The watershed has an area of around 25km^2 and a catchment length of 7.14km. Located in a mountainous

region, the watershed topography is quite steep with an average slope of 23.4°, which indicates that the time of concentration of this watershed is relatively small. More detailed description of the watershed characteristics can be found in Table 1.

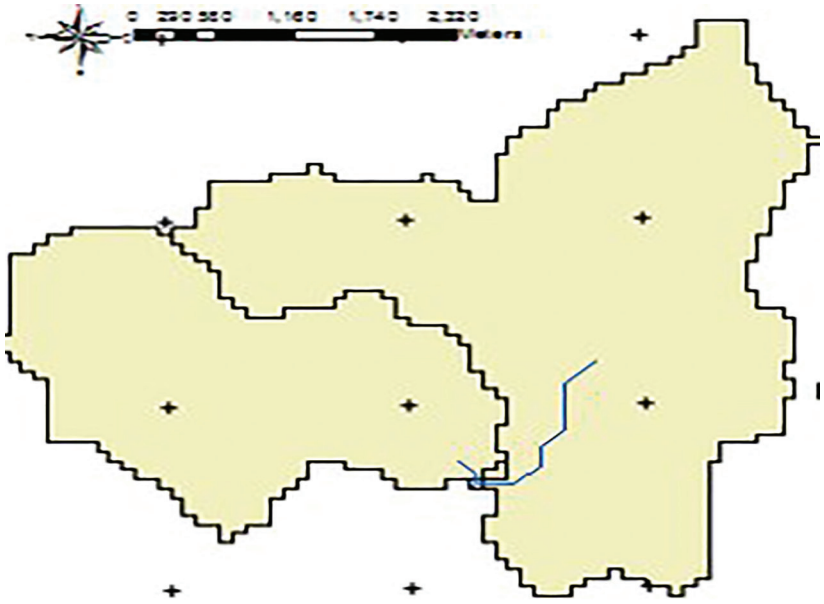

Figure 1. Watershed of Tong Soong Bridge

Table 1. Characteristics of Tong Soong watershed

No.	Characteristic	Symbol	Unit	Value
1	Design probability	P	%	2
2	Catchment area	A	km^2	19.48
3	Main flow length	L	km	1.8
4	Catchment length	Llv	km	7.03
5	Catchment averaged width	B	km^2/km	2.77
6	Catchment roughness			2.00
7	Catchment averaged slope	Sb	%	25.15
8	River bed slope	Sr	%	0.05

4.1 Determination of design hyetographs

In order to develop the design hydrograph for Toong song watershed, we collected hourly data over the period from 1975 to 2016 at Lang Son rain gauge. Subsequently, we determined the main rainfall events occurring over the 1975-2016 period and classified these events into two groups: events with total amount of 24-h rainfall lower than 100 mm (Type I) and events with 24-h rainfall higher than or equal to 100 mm (Type II). Figures 2a and 3a show the 24-hour dimensionless cumulative hyetographs of rain events 24-h rainfall lower and greater than 100mm, respectively. Based on these hyetographs, we selected the typical hyetograph of each group as shown in figures 2b and 3b. Figures 2c and 3c show the typical incremental hyetographs of each group. It is clearly seen that although the typical hyetographs of two groups are similar, the peak rainfall of type II is much higher than that of type I. Next, the design 24-h rainfall values with return frequencies of 1, 2, 5, 10, 25, 50 and 100 years were calculated based on 24-h rainfall datasets collected in the 1975-2016 period. Finally, the design hyetographs corresponding with the design 24-h rainfall

values were obtained by mapping from two typical hyetographs type I and II. These design hyetographs were used as the inputs for TR55 to construct the design hydrographs.

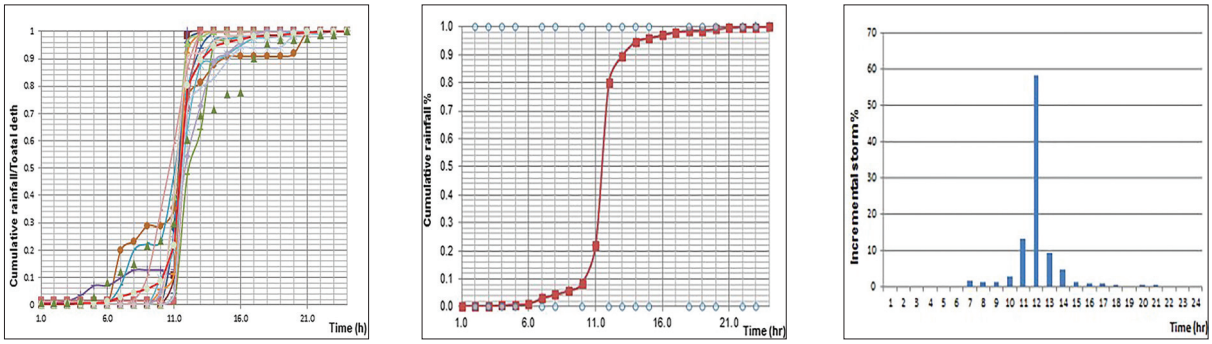

(a) *(b)* *(c)*

Figure 2. Cumulative dimensionless hyetograph and design hyetograph in Lang Son (type I)

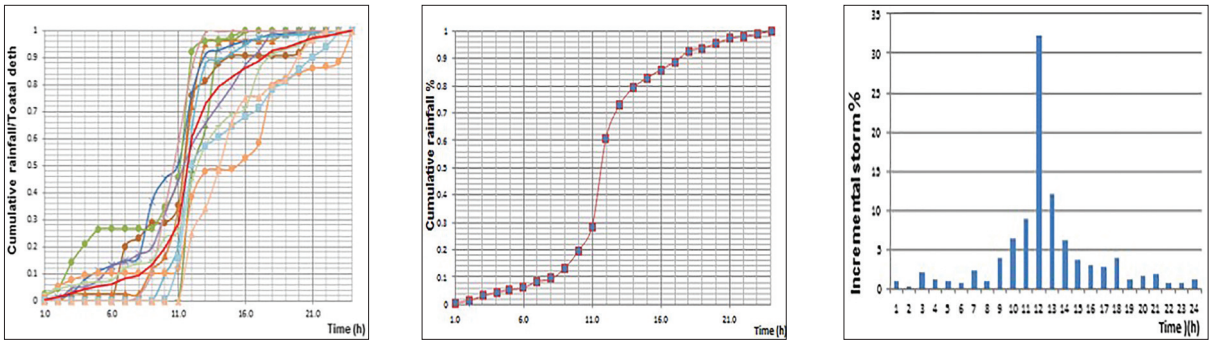

(a) *(b)* *(c)*

Figure 3. Cumulative dimensionless hyetographs and design hyetographs in Lang Son (type II)

4.2. Land use map and Curve number map

In order to estimate runoff from storm rainfall, the TR55 model uses the curve number (CN) method as mentioned in section 2. Determination of CN depends on the watershed characteristics including soil and land cover conditions, which the model represents as hydrologic soil group, land use, treatment, and hydrologic condition. Given those watershed data, the CN map can be constructed using GIS tools. Figure 4 shows the land cover and CN maps of the Toong song watershed. The figure indicates that there are three regions with CN values of 77, 71 and 70 in which the regions with CN values of 77 and 70 occupy nearly all watershed. Similar to the CN estimation, the time of concentration Tc and time of travel Tt were also calculated by GIS tool from the topography map.

4.3 Determination of design hydrograph

The 1-day hydrograph for the Tong Soong watershed was constructed from the daily rainfall with return periods of 1, 2, 5, 10, 25, 50 and 100 years using the TR55 method. Figure 5 shows an example of the design hydrograph at the outlet of the watershed corresponding with a return period of 50 years. Table 2 summaries the peak discharge and peak time at sub-basin, reaches and outlet of the watershed.

4. Conclusions

In this study, the TR55 method was explored and applied to estimate the designed hydrographs with return periods from 1 to 100 years. The initial results show that this method is suitable for calculation of designed hydrograph for small and medium watershed. Particularly, the calculation of time of concentration using this method, which accounts for the time traveling both on hill slope and on the river, is more accurate than the traditional methods. The accuracy of runoff simulation using combined GIS and TR55 was

also confirmed in the study of Ramana (2014). The application of the TR55 method shows a great potential to derive hydrographs and develop a database of hyetographs and hydrographs for other mountainous regions having similar conditions in Northern Viet Nam. However, care should be taken as the procedures in TR-55 are simplified by assumptions about some parameters. These simplifications, however, limit the use of the procedures and can provide results that are less accurate than more detailed methods. The user should examine the sensitivity of the analysis being conducted to a variation of the peak discharge or hydrograph when using the method.

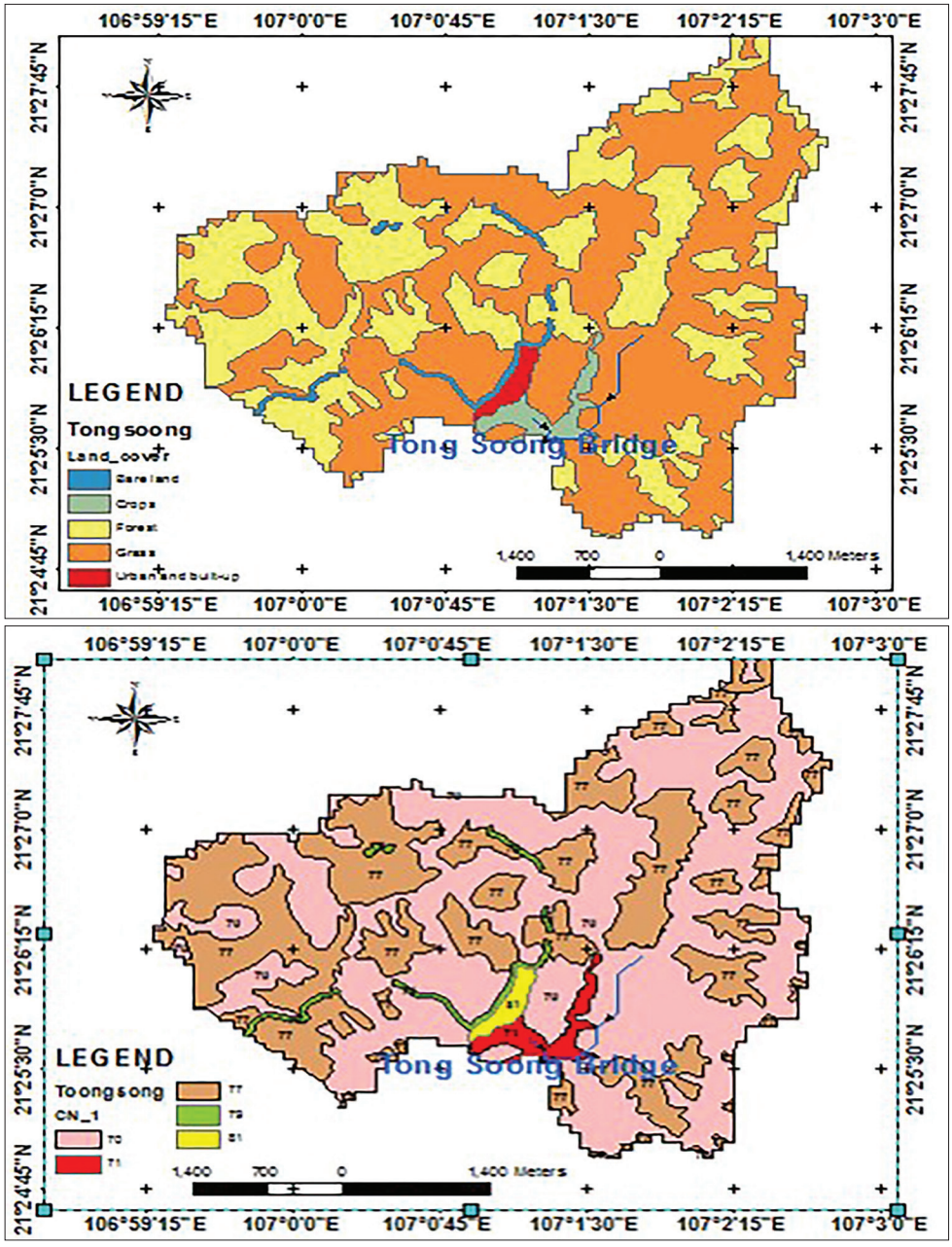

Figure 4. Land cover and Curve number map in Tong Soong

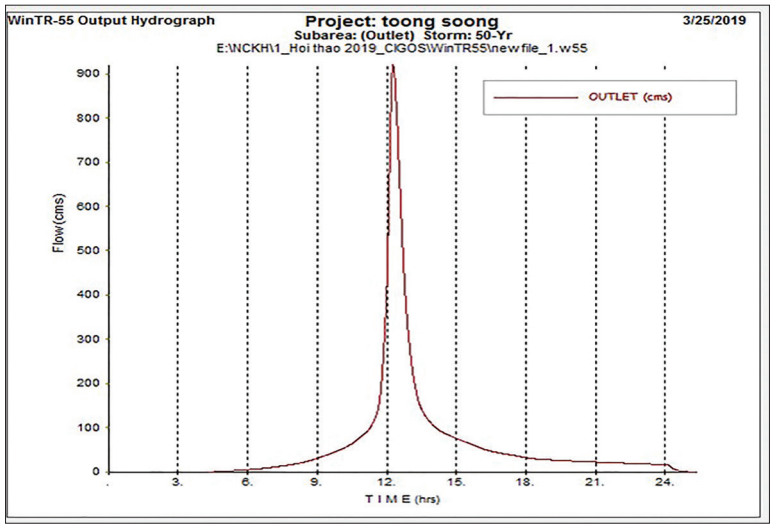

Figure 5. Design hydrograph at Tong Soong watershed

Table 2. Flood peak with different return periods at Tong Soong

Region: lang son Locale:

Hydrograph Peak/Peak Time Table

Sub-Area or Reach Identifier	Peak Flow and Peak Time (hr) by Rainfall Return Period 2-Yr (cms) (hr)	5-Yr (cms) (hr)	10-Yr (cms) (hr)	25-Yr (cms) (hr)	50-Yr (cms) (hr)	100-Yr (cms) (hr)	1-Yr (cms) (hr)
SUBAREAS							
sub 1	75.86	82.05	228.38	306.51	364.87	422.24	72.04
	12.16	12.16	12.16	12.15	12.16	12.15	12.17
sub 2	118.94	128.36	359.06	483.43	574.75	666.47	112.36
	12.24	12.23	12.24	12.21	12.23	12.21	12.22
sub 3	0.40	0.44	1.20	1.60	1.90	2.20	0.38
	12.13	12.13	12.12	12.12	12.12	12.12	12.13
REACHES							
reach 1	75.86	82.05	228.38	306.51	364.87	422.24	72.04
	12.16	12.16	12.16	12.15	12.16	12.15	12.17
Down	75.85	82.02	227.80	306.06	363.75	421.67	71.85
	12.26	12.26	12.23	12.22	12.21	12.22	12.24
reach 2	118.94	128.36	359.06	483.43	574.75	666.47	112.36
	12.24	12.23	12.24	12.21	12.23	12.21	12.22
Down	118.75	128.27	358.49	482.76	574.12	665.18	112.36
	12.38	12.36	12.30	12.32	12.30	12.31	12.36
OUTLET	188.93	204.11	575.62	773.54	921.49	1068.16	178.92

References

1. Chow V.T: Applied Hydrology (1988), *In: Hydrology-572 pages*.
2. Chow V.T (1964), *Handbook of Applied Hydrology*.
3. Le Van Nghinh (2000), *Hydrological principles. Agricultural Publishing Inc.*
4. Le Dinh Thanh (1996), *Estimation of PMP and PMF for Vietnam. PhD Dissertation. Hanoi Water University.*
5. Ngo Le Long (2015), *Study on scientific basics for proposing standards of designed flood, sea dykes in the context of climate change, sea level rise in Viet Nam and mitigation measures*.
6. Ramana, G.Venkata, (2014), *Rainfall runoff modelling between TR-55 hydrologic watershed model and overland time of concentration model. A RAMANA, International Journal of Advances in Computer Science and Technology,* 3(3).
7. United States Department of Agriculture, (1999), *Urban Hydrology for Small Watersheds*.

GREENHOUSE GAS EMISSIONS IN AGRICULTURE, BUILDINGS AND WASTER SECTORS IN HO CHI MINH CITY

Le Anh Ngoc[(1)], Nguyen Van Tin [(1)], Pham Duc An [(1)], Vo Thi Nguyen[(1)], Bao Thanh[(2)]
[(1)]*Sub-Institute of Hydrometeorology and Climate Change*
[(2)]*Ho Chi Minh University of Natural Resources and Environment*

Received: 15 February 2019; Accepted: 2 March 2019

Abstract*: Climate change (CC) is a common problem for all people with a strong influence on the world. One of the main causes of climate change is greenhouse gases (GHG). Viet Nam has implemented the National greenhouse gas inventories for five sectors: agriculture, energy, industrial processes, waste, land use change and forestry. Being the biggest economic development centre in Viet Nam, Ho Chi Minh City has emitted numerous amounts of greenhouse gases every year. This paper presents results of GHG calculations in agriculture, waste and buildings in Ho Chi Minh City applying the 2006 IPCC guideline. It is found that greenhouse gases in Ho Chi Minh were about 1.1 million, 3 million and 0.4 million tons of CO_2 equivalent in agriculture, waste and buildings, respectively.*

Keywords*: IPCC Guideline 2006, greenhouse gas inventory for agriculture, waste, buildings.*

1. Overview of agriculture, waste and buildings sectors in Ho Chi Minh City

1.1 Agriculture

Crop Cultivation: Crop structure continues to reduce rice area while increases area of flower, safe vegetables, fodder grass and other annual industrial crops. By 2013, the total area of rice cultivation in the city was about 29,293 hectares. According to the master plan to 2020, rice area will reduce to 3,200 ha.

Livestock: By 2020, the number of dairy cows and pigs are expected at 75,000 heads, 25,600 heads, 800 heads and 275,000 heads, respectively.

Aquaculture: Area of saltwater aquaculture was about 8,460 ha, concentrating mainly in Can Gio and 1,640 ha of freshwater fisheries, mainly in Binh Chanh and Cu Chi Districts. The farming area by 2020 according to the planning has not changed. [2]

1.2 Waste

Thee volume of domestic solid waste was brought to landfills and solid waste treatment plants in the city estimate about 8,300 tons/day.

However, domestic solid waste has not been classified at source, causing great pressure on treatment facilities. Solid waste treatment technology is mainly landfill method (about 75% of the total volume), the rate of solid waste treated by compost processing method was about 15%, the rate of solid waste is treated by burning technology was about 5-10%.

The wastewater sector includes domestic wastewater, medical waste water and industrial wastewater. Regarding domestic wastewater, the amount of urban wastewater was about 2.75 million tons/day, of which 13% was treated. Wastewater from health facilities was around 17,750m^3/day, industrial wastewater from 13 industrial parks, 3 export processing zones and 33 production facilities is about 278,191m^3/day.

In the situation of increasing waste and impacts of climate change, Ho Chi Minh City needs a master plan to deal with substances of which clearly defining the scale and location of waste treatment facilities. The buildings investment roadmap and technology

Corresponding author: Le Anh Ngoc
E-mail: leanhngoc.sihymecc@gmail.com

in each stage must be specifically set up to keep up with the city's development speed.

1.3. Buildings

Total of high-rise buildings in 2013 in Ho Chi Minh City is 452 piles including 126 projects in district 1, 107 projects in district 7, 66 projects in district 3, 24 projects in district 2. The total electricity consumption for these buildings was 725 million KWH, in which district 1 consumed about 385 million KWH, accounting for 52%. The total electricity consumption for the facilities accounted for 4% of the city's total electricity consumption.

2. Data and research methods

2.1 Database

2.1.1. Agriculture

Data in the agriculture sector was collected from the Department of Agriculture and Rural Development of Ho Chi Minh City.

2.1.2. Domestic solid waste

Nowadays, Ho Chi Minh City Urban Environment Company is mainly responsible for collecting the solid waste amount. All domestic solid waste is treated by two main methods, namely burial and compost production, where concentrated in Da Phuoc and Tay Bac Cu Chi treatment areas (Landfill No. 2, Vietstar Company). Of which, burial method accounts for about 85%, whereas compost is about 15%.

Table 1. Composition of Domestic solid waste in Ho Chi Minh City

Composition	%
Paper	2.8
Garbage	0
Food	67.9
Wood/ Straw	0.06
Textile	6.4
Skin	2.24
Others	20.6
Total	100

(Source: Department of Solid Waste Management, Department of Natural Resources and Environment of Ho Chi Minh City)

Table 2. Volume of treated domestic solid waste

Types	Volume (tons/year)	Volume (tons/day)	Rate %
Landfill	2,007,135	5,499	80
Burning	146	400	6
Compose	327,040	896	13
Recycle	19,710	54	1
Total	2,499,885	6,849	100

2.1.3. Wastewater

According to survey information of Saigon University, processing technology of EPZs / IPs in Ho Chi Minh City was all Aerotank and SBR forms. These technologies treat wastewater by biological methods under aerobic conditions. Although the centralized wastewater treatment systems of EPZs/IPs are managed and operated relatively methodically, the treatment efficiency has not been as expected, so the group chose MCF = 0.2 to calculate emissions.

Table 3. Wastewater composition of industrial zones and export processing zones in Ho Chi Minh City

No.	KCN-KCX	Actual capacity (m^3/day)	BOD5	COD	N-Total	TSS	Coliforms
1	An Ha	1,100	51	70	12.6	236	12,000
2	Binh Chieu	350	354	632	114	196	4.6x106
3	Cat Lai II	2,400	185	330	18.2	105	9x105
4	Vinh Loc	4,600	200	600	60	300	5,000-8,000
5	Hiep Phuoc	3,500	100	400	60	200	-
6	Cu Chi	3,100	60	109	26.8	82	2x104
7	Le Minh Xuan	9,800	150	600	60	200	-
8	Linh Trung	2,000	500	800	30	300	104
9	Linh Trung II	1,700	-	225	73.50	122	-
10	Tan Binh	4,200	55-135	105-280	16.27	59	1,500-3,000
11	Tan Phu Trung	2,300	198	325	39.6	215	104
12	Tan Tao	1,500	220	500	40	220	105-106
13	Tan Thoi Hiep	5,000	576	1,384	39.7	300	-
14	Tan Thuan	400	88	135	32.8	92	4.6x104
15	Dong Nam	30	Trial operation				
16	Hoa Phu	80	Under buildings				

2.1.3. Buildings

Data for buildings was collected from Department of Construction.

2.2. Methods

2006 IPCC Guidelines for Greenhouse Gas Inventories were applied to calculate GHG for the three sectors in Hochiminh City, as follows:

2.2.1. Agriculture

The method identifies emission of GHG mainly CO_2, CH_4, N_2O through emission factors in each field and industry. These emission factors are included in the IPCC emission calculation formulas for each category of greenhouse gases.

- Rice Cultivation: Annual CH_4 emission from rice

$$CH_{4Rice} = A * t * EF_i * 10^{-6} \quad (1)$$

Where: CH_{4Rice}= Annual CH_4 emission from Rice Cultivation (Gg CH_4 yr-1), EF_i: Adjusted daily emission factor for a particular harvested area (kg CH_4 ha-1 day-1), t = Cultivation period of rice (day), A = Annual harvested area (ha yr-1).

- Livestock:

In this article, greenhouse gases in livestock generated from the intestinal fermentation of livestock and manure management process were calculated.

Methane Emissions from Enteric Fermentation

$$CH_4 Enteric = N(T) * EF(T) * 10^{-6} \quad (2)$$

Where: CH_4 Enteric= Emission factor for Enteric Fermentation (Gg CH_4 yr-1), N (T)= Number of animals (head), EF(T)= Emission factor for Enteric Fermentation (kg head-1 yr-1).

Table 4. Emission factor for Enteric Fermentation

Category of animal	EF(T) (kg head-1 yr-1)
Dairy Cattle	61
Other Cattle	47
Buffalo	55
Swine	1

Methane Emissions from Manure Management

$$CH_4\ Manure = N\ (T) * EF\ (T) * 10^{-6} \quad (3)$$

Where: CH_4 Manure= CH_4 emissions from Manure Management (Gg CH_4 yr-1), EF(T)=Emission factor for Manure Management (kg head-1 yr-1), N (T)= Number of animals (head).

Table 5. The coefficient of methane emission from faeces of some livestock [4]

Category of animal	26°C	27°C	>28°C
Dairy Cattle	28	31	31
Other Cattle	1	1	1
Buffalo	2	2	2
Swine	6	7	7

Direct N_2O Emissions from Manure Management Systems

$$N_2O\ (mm) = NEMMS * EF3(S) * 44/2 \quad (4)$$

Where: N_2O (mm)= Annual direct N_2O emissions from Manure Management (kg N_2O yr-1), NE_{MMS}=Total nitrogen excretion for the MMS (kg N yr-1), EF3(S)=Emission factor for direct N_2O-N emissions from MMS [kg N_2O-N (kg N in MMS)-1], 44/28 =conversion of (N_2O-N) (mm) emissions to N_2O(mm) emissions

Table 6. Default values for nitrogen excretion rate in Asia (kg n (1000 kg animal mass) -1 day-1)

Category of animal	Nrate (kgN/ton/day)	TAM (kg/head)
Dairy Cattle	0.47	350
Other Cattle	0.34	200-275
Swine	0.42	60
Buffalo	0.32	350-550

$$Nex_{(T)} = Nrate(T) * TAM * 10\text{-}3 * 365 \quad (5)$$

Where: $Nex_{(T)}$=Annual N excretion per head of species/livestock category (kg N animal-1 year-1), Nrate(T)= Default N excretion rate [kg N (1000 kg animal)-1 day-1], TAM= Typical animal mass for livestock category (kg)

Amount of manure nitrogen that is loss due to volatilisation of NH_3 and NO_x

$$V_{olatilization\text{-}MMS} = NE_{MMS} * Frac_{(GasMS)} \quad (6)$$

Where: NE_{MMS}=Total nitrogen excretion for the MMS, $Frac_{GasMS}$=Fraction of managed livestock manure nitrogen that volatilises (Dairy Cattle =40%, Other Cattle =45%, Buffalo =25%, Swine =45%.)

- *Aquaculture:*

$$CH_4\ EmissionWWflood = P * E(CH_4)diff * Aflood\_\ total\ surface * 10\text{-}6 \quad (7)$$

Where: $CH_{4\ EmissionsWWflood}$=Total emission CH_4 from flood surface ($GgCH_4$ yr-1); P: time, day yr-1; $Af_{lood\_\ total\ surface}$=Annual flood total surface area (ha).

2.2.2. Domestic solid waste

Formula to calculate greenhouse gas emissions from landfills:

$$Lo = Wx\ MCF \times DOC \times DOCF \times (16/12)\ xF \quad (8)$$

Where: Lo = CH_4 generation potential, Gg; W = mass of waste deposited, Gg; DOC = degradable organic carbon in the year of deposition, fraction, Gg C/Gg waste; DOCf = fraction of DOC that can decompose (fraction); MCF = CH_4 correction factor for aerobic decomposition in the year of deposition (fraction); DOC, Gg F = fraction of CH_4 in generated landfill gas (volume fraction) 16/12 = molecular weight ratio CH4/C (ratio).

Formula to calculate greenhouse gas emissions from biological waste treatment by biological method

*CH_4 emissions from biological treatment

$$CH_4\ Emissions = \sum_i (M_i \times EF_i) \times 10^{-3} \text{-} R \quad (9)$$

Where: CH_4 Emissions=total CH_4 emissions in inventory year, Gg; CH_4 Mi=mass of organic waste treated by biological treatment type i, Gg; EF=emission factor for treatment i, g CH_4/

kg waste treated; i=composting or anaerobic digestion; R=total amount of CH_4 recovered in inventory year, Gg CH_4.

*N_2O emissions from biological treatment

$$N_2O\ Emissions = \sum_i (M_i \times EF_i) \times 10^{-3} \quad (10)$$

Where: N_2O Emissions=total N_2O emissions in inventory year, Gg N_2O; Mi=mass of organic waste treated by biological treatment type i, Gg; EF=emission factor for treatment i, g N_2O/ kg waste treated; i=composting or anaerobic digestion;

Formula to calculate greenhouse gas emissions from burning solid waste by burning method

$$E_{j,f} = M_f * EF_{j,f} \quad (11)$$

Where: $E_{j,f}$=Gas discharge load j of the type of fuel f used during combustion, (ton); M_f=Fuel consumption type f, (TJ); $EF_{j,f}$=Gas emission factor default j of f fuel type (ton/TJ); J:Type of exhaust gas; F: The type of fuel used during combustion/firing.

2.2.3. Wastewater

Greenhouse gases in the field of wastewater management in Ho Chi Minh City include emissions from wastewater treatment activities. Formula to calculate greenhouse gas emissions in the field of wastewater management:

$$CO_2 = Q \times BOD_5 \times B_0 \times MCF \times GWP\_CH_4 \quad (12)$$

Where: Q: wastewater flow (m3/day);

BOD_5: country-specific per capita BOD in inventory year, g/person/day;

B_0 = maximum CH_4 producing capacity, kg CH_4/kg BOD (0,6kgCH_4/kg BOD);

MCF = methane correction factor (fraction)

2.2.4. Buildings

Method of calculating greenhouse gas emissions for energy consumption

$$E_{CO2} = M * EF_e \quad (13)$$

Where: M: Total of Electric energy consumption (MWH); EF_e: Emission factor of electricity (EF_e= 0.56 TCO_2/MWH from the Department of Meteorology, Hydrology and Climate Change)

3. Results and Discussions

3.1. GHG emissions in Agriculture

According to the calculation results, CO_2 emissions in the agricultural sector in 2013 was about 1.16 million tons of CO_2eq, of which emissions from livestock accounted for the majority. The forecast according to the plan until 2020 emissions will be reduced to about 800 thousand tons of CO_2 equivalent.

Table 7. Total CO_2 emissions in the agricultural sector

Field	2013	2020
Cultivation	243,273	73,125
Livestock	830,662	652,452
Aquaculture	85,274	77,785
Agriculture	1,159,209	803,362

3.2. Greenhouse gas emissions in the waste sector

Solid waste sector

Total emissions in the solid waste sector in Ho Chi Minh City was 2,764,212.52 tons of CO_2, of which emissions mainly from landfills, followed by emissions from biological methods.

Waste water

Total GHG emissions from the wastewater treatment sector in Ho Chi Minh City 143,347.9 tons of CO_2 equivalent, emissions mainly from industrial wastewater emit 81,973 tons of CO_2 (accounting for 57.2%), emissions from untreated domestic wastewater are about 58,945.2 tons of CO_2 (41.1%).

3.3. Greenhouse gas emissions in the buildings sector

Total GHG emissions in 2013 in high-rise buildings in Ho Chi Minh City was 406,294 tons of CO_2, corresponding to electricity consumption of over 700 million KWH. District 1 was the largest emission (53.2%), where most of the office buildings and large commercial centres are located. The second and the third were District 7 and District 3, accounting for 15.8% and 9.1%, respectively.

Table 8. Total CO_2 emissions (tons of CO_2) in the solid waste sector

Treatment	Landfill	Compost	Burning	Total
CO_2 eq. yr -1	2,750,275	110,610	2,876.52	2,764,212.52

Table 9. Total volume of wastewater in 2016 in Ho Chi Minh City

Type of treatment	CO2 eq. yr -1	Rate (%)
Domestic wastewater	58,945.2	41.1
Aerobic treatment	0	0
Untreated	58,945.2	41.1
Medical waste water	2,429.5	1.7
Industrial Wastewater	81,973.2	57.2
Total	**143,347.9**	**100**

4. Conclusion

In the context of the developing economy, the calculation of GHG emissions contributes to develop Ho Chi Minh's economy while reducing the risk of climate change in agriculture, waste and buildings sectors based on 2006 IPCC guidelines for GHG Inventory and data from relevant authorities.

In agricultural sector, there was about 1.1 million tons of CO_2 in 2013, in which, the largest emission was from livestock (71.7%), followed by cultivation (21%) and the least emission was from aquaculture (7.4%). Main proposed technical measures to decrease GHG in livestock includes reducing CH_4 emissions from the intestinal tract, add starch to plant fibre in diets, providing MUB nutrition cake (Molasses Urea Block) for dairy cows.

Total emissions in the waste industry in Ho Chi Minh City were about 3 million tons of CO_2 equivalent, of which 2,863,761 CO_2eq (95,2%) in the solid waste sector and 143,348 CO_2 eq (4,8%) in wastewater treatment. Major actions have been implemented in Ho Chi Minh City for decreasing GHG in solid waste such as encouraging CH_4 fermentation technology with combined with electricity generation, developing policies to support recycling actions or reducing solid waste amount treated by disposal sites or burning.

In the buildings sector, the amount of greenhouse gas emissions was 406,294 tons of CO_2 equivalent from the consumption of more than 700 million KWH for buildings. Some solutions to decrease emissions consist of applying Building Energy Management System in buildings to increase energy savings, using air conditioners and refrigerators with high energy efficiency in households, implementing energy-saving solutions in lighting systems.

References

1. Ministry of Agriculture and Rural Development (2011), *Scheme on GHG emission reduction in Agriculture and Rural Development by 2020.*
2. Le Viet Bao (2014), *Situation of agricultural production in the area of Ho Chi Minh City 2011-2014*, Department of Agriculture and Rural Development of Ho Chi Minh City.
3. Nguyen Van Tinh, Nguyen Quang Trung, Nguyen Viet Anh (2007), "Influence of methane wastewater regime in the field drying periods", *Journal of Science and Technology*.
4. *2006 IPCC Guidelines for National Greenhouse Gas Inventories, Vol4 Agriculture, Forestry and Other Land Use.*
5. *2006 IPCC Guidelines for National Greenhouse Gas Inventories, Vol5 Waste*.

IMPACT OF SATELLITE OBSERVED SST ON INTENSITY AND TRACK SIMULATION OF TROPICAL CYCLONE OVER VIET NAM EAST SEA: A CASE STUDY OF TYPHOON NALGAE (2011)

Nguyen Thi Thanh[(1)], Nguyen Xuan Hien[(1)], Hoang Duc Cuong[(2)]
[(1)]*Viet Nam Institute of Meteorology Hydrology and Climate Change*
[(2)]*The National Centre for Hydro-Meteorological Forecasting*

Received: 18 February 2019; Accepted: 1 March 2019

Abstract: *Sea surface temperature (SST) is one of the most important thermal factors affecting typhoon. This paper was carried out to examine the impact of satellite observed SST on intensity and track simulation of tropical cyclone over Viet Nam East sea by using the Weather Research and Forecast (WRF) model. We have selected typhoon Nalgae (2011) for studying the SST impact. Three different sets of SSTs were used in this study: (1) SST from GFS analysis is provided for the initial condition and kept unchanged during the 72 hr simulation; (2) SST from Remote Sensing Systems (RESS) is used for the initial condition and kept unchanged during the 72 hr simulation; (3) SST from RESS is updated every 24 h for the initial and boundary conditions. The simulated results show that the using SST from satellite data for both only initial condition case and initial and boundary conditions case significantly improve the simulated intensity of typhoon due to improved simulation of latent heat and heat fluxes.*

Keywords: *Sea surface temperature, SST, typhoon, tropical cyclone, the Viet Nam East Sea*

1. Introduction

It has been recognized that the Sea Surface Temperature (SST) is one of the most important parameters which plays a significant role in the formation and intensification of tropical cyclone [12, 13]. Gray (1968, 1978) noted that the 26°C isotherm deepening to a depth to 60m from the surface is required for the formation of tropical cyclone. SST determines the amount of sensible and latent heat available to the tropical cyclone from the ocean, hence, it is indicative of the intensity of tropical cyclone [12].

Large number of studies [1,5-7,14, etc] found that the intensity of tropical cyclone increases rapidly when it passes through the warm water area due to increasing the sensible and latent heat flux. Shankar et al. (2007) showed that not only the magnitude of SST but also its gradient affects surface wind and convective activity, which affects the intensity of the tropical cyclone. Studies were also performed to investigate the influence of SST on the movement of tropical cyclone. Wu (2005) studied the effect of symmetric and asymmetric SST distributions on the centre of tropical cyclone on the movement of tropical cyclone. Accordingly, the asymmetric SST distribution over large areas affected the movement of tropical cyclone due to various surface friction and surface heat flux [2]. Recently, results from numerical weather prediction (NWP) model shown that the intensity and track of simulated tropical cyclones vary with the various SST due to the changed resolution of SST fields [11,17,4].

In operational NWP modelling applications, SST field is generally obtained from GFS analysis data of National Centers for Environmental Prediction (NCEP) with

Corresponding author: Nguyen Thi Thanh
E-mail: thanhnt.met@gmail.com

horizontal resolution of 0.5° x 0.5°. There is a need for alternative SST datasets, which can give more accurate representation of ocean boundary condition in the NWP model.

Nowadays, SST products are available from microwave (MW) and infrared (IR) sensors. One of these is the SST product from Remote Sensing Systems (RESS), Northern California, American. It is created from Tropical Rainfall Measuring Mission Microwave Imager (TMI), Advanced Microwave Scanning Radiometer (AMSR-E), Advanced Microwave Scanning Radiometer 2 (AMSR2), WindSat and the Moderate Resolution Imaging Spectroradiometer (MODIS) data. This SST data is the daily optimally interpolated product at 9 km x 9 km (MW_IR OI SST). Thus, it can be seen that MW_IR OI SST data is higher horizontal resolution than GFS SST data.

The objective of the present study is to investigate the impact of MW_IR OI SST on intensity and track simulation of tropical cyclones by using Weather Research and Forecast (WRF) model.

2. Data, experimental design and methodology

2.1. Data

The MW_IR OI SST is available at website: http://www. remss.com/.

The GFS analysis data of National Centres for Environmental Prediction available at 0.5° x 0.5° horizontal resolution and 6 hourly interval has been interpolated to the model grid for providing the initial and boundary conditions. This data is provided at website: ftp://nomads.ncdc.noaa.gov/GFS/analysis_only/.

In addition, tropical cyclone best track data (including tropical cyclone centre locations and intensities) from IBTrACS (International Best Track Archive for Climate Stewardship) data of National Oceanic and Atmospheric Administration (NOAA) and National Climatic Data Center (NCDC) has been used to verify the model simulated track and intensity from two different experiments. This data is available in the website: https://www.ncdc. noaa.gov/ibtracs/.

2.2. Experimental design

The mesoscale model used in this study is the WRF model version 3.6 with two nested domains. The first domain ranges from 0°N -31°N and 92°E-130°E with 135×158 grid points, horizontal resolution of 27 km. The second domain ranges from 5°N-25°N and 100°E-120°E with 259 × 250 grid points and horizontal resolution of 9 km (Fig. 1). The physics options of WRF model used the same for both domains, include the Kain–Fritch 2 cumulus parameterization scheme [10], Thompson microphysics scheme [16], Yonsei State University (YSU) [7] Planetary boundary layer scheme. Long-wave radiation and short-wave radiation are parameterized using RRTMG [8] scheme. Land surface are parameterized using the multi-layer Noah land surface model [3], and for Surface Layer, Revised MM5 Monin-Obukhov scheme [9] is used.

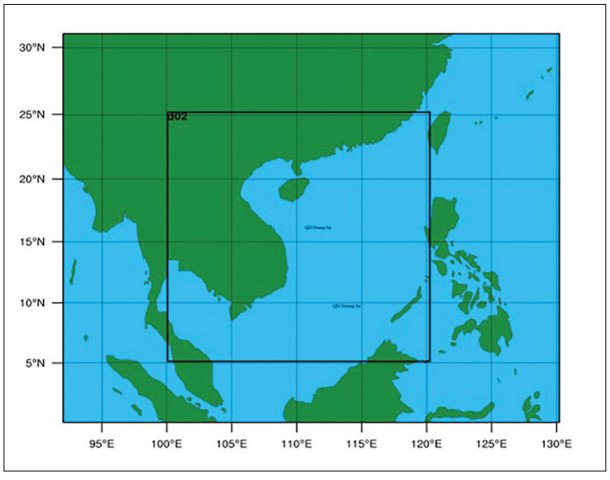

Figure. 1 The WRF model domains for cyclone simulation

Three experiments are carried out: (1) GFS SST is provided for the initial condition and kept unchanged during the 72 hr simulation (GFS); (2) MW_IR OI SST is used for the initial condition and kept unchanged during the 72 hr simulation (SSTVT); (3) MW_IR OI SST is updated every 24 h for the initial and boundary conditions (SSTUP).

2.2. General description of Typhoon Nalgae

Nalgae formed as a tropical depression over the Philippine Sea on September 27, 2011 and moved generally westwards. Within three days, it had strengthened into a severe typhoon. On October 1, Nalgae peaked intensity with an estimated maximum sustained wind of 175km/h, about 300 km northeast of Manila. Then it crossed Luzon and entered the Viet Nam East sea in the late afternoon. It moved west to west-north-westwards and weakened into a severe tropical storm on October 2. It weakened further into a tropical storm on 4 October and crossed the southern part of Hainan Island that afternoon and weakening into a tropical depression at night. Nalgae moved south-westwards across the southern part of the Gulf of Tonkin on October 5 and dissipated over the seas near Nghe An (Fig. 2). Due to the effect of Nalgae typhoon combined with cold front, the North East, North Central and Mid-Central regions had rainfall and heavy rainfall. The total rainfall of two days from October 4 to October 6 was commonly from 50 to 70mm, especially in the Nghe An - Ha Tinh areas, rainfall measured over 100mm.

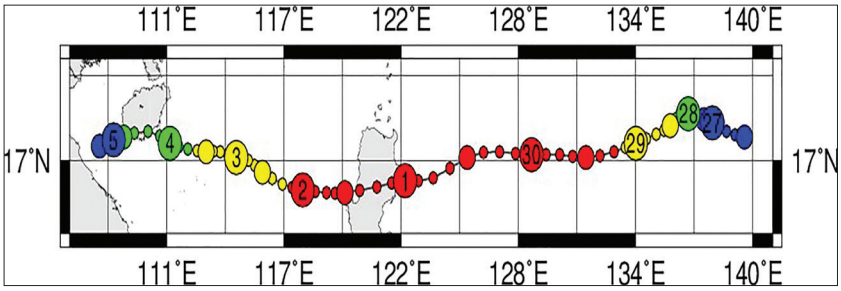

Figure. 2 Best track of Nalgae typhoon
(Source: http://agora.ex.nii.ac.jp/digital-typhoon/)

3. Results and discussion

The simulation of Nalgae typhoon for GFS, SSTVT and SSTUP cases were initialized at 00Z on October 2, 2011.

Figure 3 and 4 show the comparison of the GFS SST and the MW_IR OI SST valid for October 2, 2011. Accordingly, MW_IR OI SST shows colder than GFS SST of 1° to 2°K in the North-eastern part of Viet Nam East sea due to the effect of cold front. On October 3 and 4, MW_IR OI SST shows the effect of cold front on SST field is extended to the southern (Figure 5 and 6). On October 5, the effect of cold front on MW_IR OI SST tends to decrease (Figure 7).

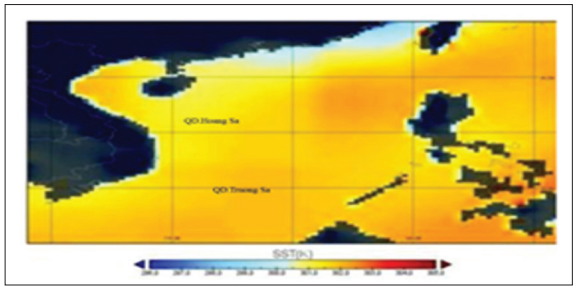

Figure. 3 SST from GFS valid for October 2, 2011

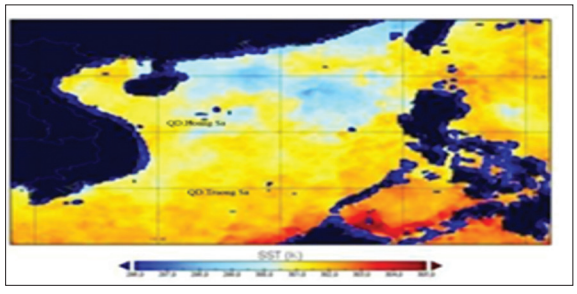

Figure. 4 SST from RESS valid for October 2, 2011

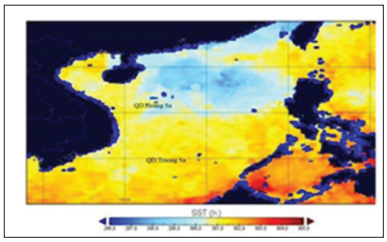

Figure 5. SST from RESS valid for October 3, 2011

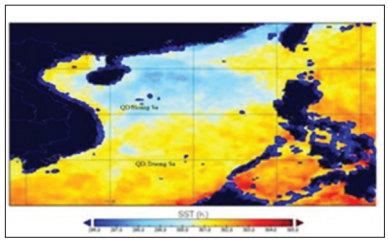

Figure 6. SST from RESS valid for October 4, 2011

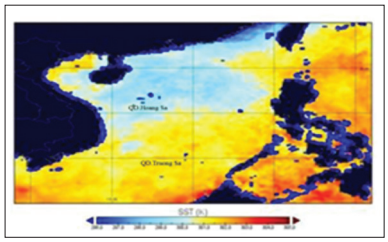

Figure 7. SST from RESS valid for October 5, 2011

Figure 8 shows that there is significant difference in the simulated latent heat fluxes between SSTVT and GFS cases. The 24 hr simulated latent heat flux in SSTVT relatively decreases in both area and magnitude when compared to GFS case. In the centre of Nalgae, the latent heat flux in SSTVT is smaller upto 400 Wm-2 than in GFS (Figure 8 a and d). For 48 and 72 hr, the difference in latent heat fluxes between GFS and SSTVT is relatively clear, especially in the southwestern part of the centre of Nalgae typhoon (Figure 8 b, c and e, f). The simulated latent heat fluxes is not much difference between SSTVT and SSTUP cases for 24 hr, 48 hr and 72 hr simulations (Figure 8 d, e, f and g, h, i).

During the 72 hr simulation, the simulated sensible heat fluxes in SSTVT is also relatively smaller when compared to GFS case and it is not much difference when compared to SSTUP case (Figure 9).

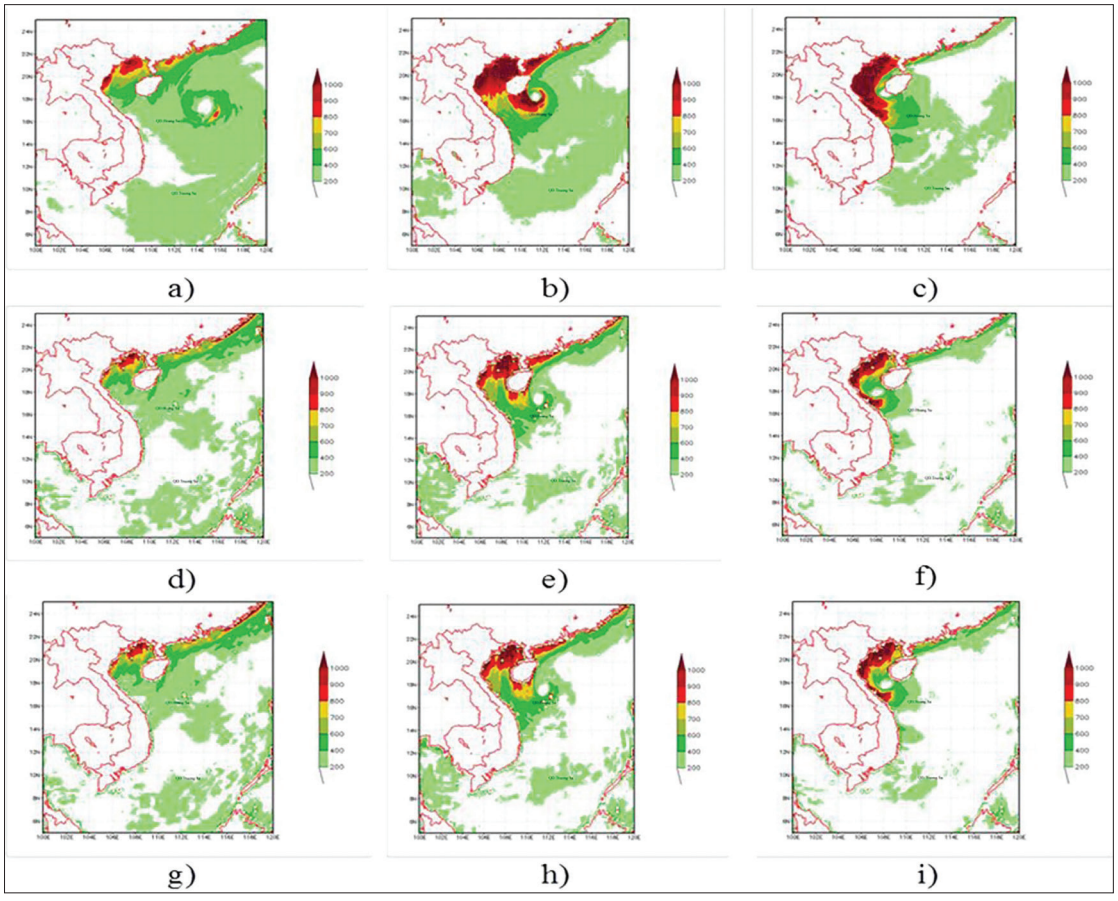

Figure 8. The simulated latent heat flux (Wm-2) after 24 hr (a, d, g), 48 hr (b, e, h) and 72 hr (c, f, i) from 00 Z on July 30, 2013 for: GFS (a,b,c) case; SSTVT (d, e, f) and SSTUP (g, h, i) case

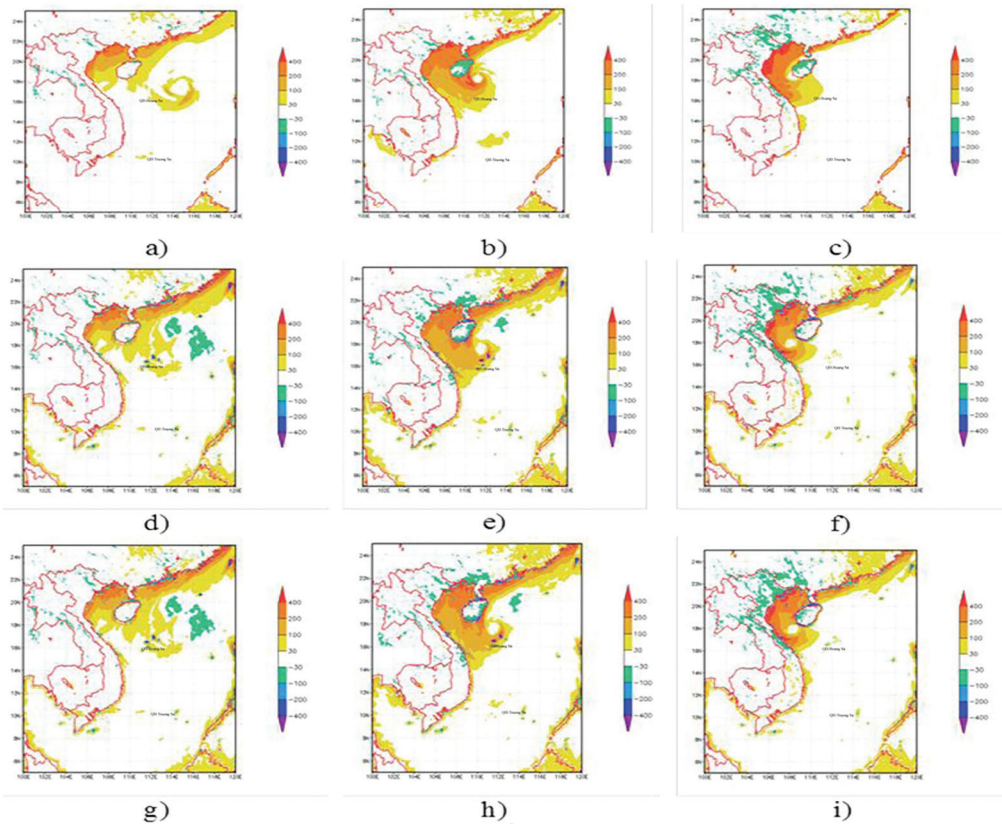

Figure 9. The simulated sensible heat flux (Wm-2) after 24 hr (a, d), 48 hr (b, e) and 72 hr (c, f) from 00 Z on July 30, 2013 for: GFS (a,b,c); SSTVT (d, e, f) and SSTUP (g, h, i) cases

Figure 10 shows the simulated sea level pressure and the wind velocity at 10 m after 24 hr (a, d, g), 48 hr (b, e, h) and 72 hr (c, f, i) from 00 Z on October 2, 2011 for GFS (a, b, c); SSTVT (d, e, f) and SSTUP (g, h, i) cases. The simulated sea level pressures and the wind velocities at 10 m for GFS demonstrate the intensity of Nalgae typhoon is strengthened from 24 hr to 48 hr simulations and significantly decreases at 72 hr simulation (Figures 10 a, b, c). On the Figures 10 d, e, f and g, h, i show the intensity of Nalgae typhoon slight increases from 24 hr to 48 hr simulations and significantly decreases at 72 hr simulation. Figure 10 also shows the simulated sea level pressures increases and the wind velocities at 10 m relatively decreases in both area and magnitude in SSTVT than in GFS. Location of the simulated typhoon centre in SSTVT is slightly shifted toward southwestern when compared to GFS during 72 hr simulation. The updating of the MW_IR OI SST data makes the cooling of the SST field at active area of the typhoon which leads to decreasing the latent heat flux and the sensible heat flux, therefore, decreases in the intensity and changes in the location of the simulated Nalgae typhoon compared to GFS. Figures 10 also shows there are not much difference in area of the simulated sea level pressures and the wind velocities at 10m between SSTVT and SSTUP cases. However, magnitude of the simulated sea level pressures and the wind velocities at 10 m in SSTVT is slightly smaller than in SSTUP in the North enter of typhoon for 48 hr and 72 hr simulation.

Figure 11 shows the time series of intensity a) Pmin; b) Vmax for Nalgae typhoon simulated from 00 Z on October 2, 2011 by GFS, SSTVT and SSTUP cases and observed by IBTrACS. The Pmin and Vmax are overestimated the IBTrACS observation for three cases, especially after 30

hr simulation. However, SSTVT and SSTUP show significant improvement in Pmin and Vmax simulation when compared to GFS. The Vmax in SSVT is difference upto 3m/s when compared to SSTUP case. However, the Pmin is not much difference between the SSTVT and SSTUP.

Figure 12 shows the observed IBTrACS best track and simulated tracks for Nalgae typhoon from 00 Z on October 2, 2011 by SSTVT and SSTUP. Accordingly, the simulated track for GFS shifts south-eastward when compared to Best Track. However, the simulated tracks for SSTVT and SSTUP cases slightly shift south-westward when compared to Best Track. The distance error in GFS is significant smaller than the SSTVT and SSTUP cases (Figure 13).

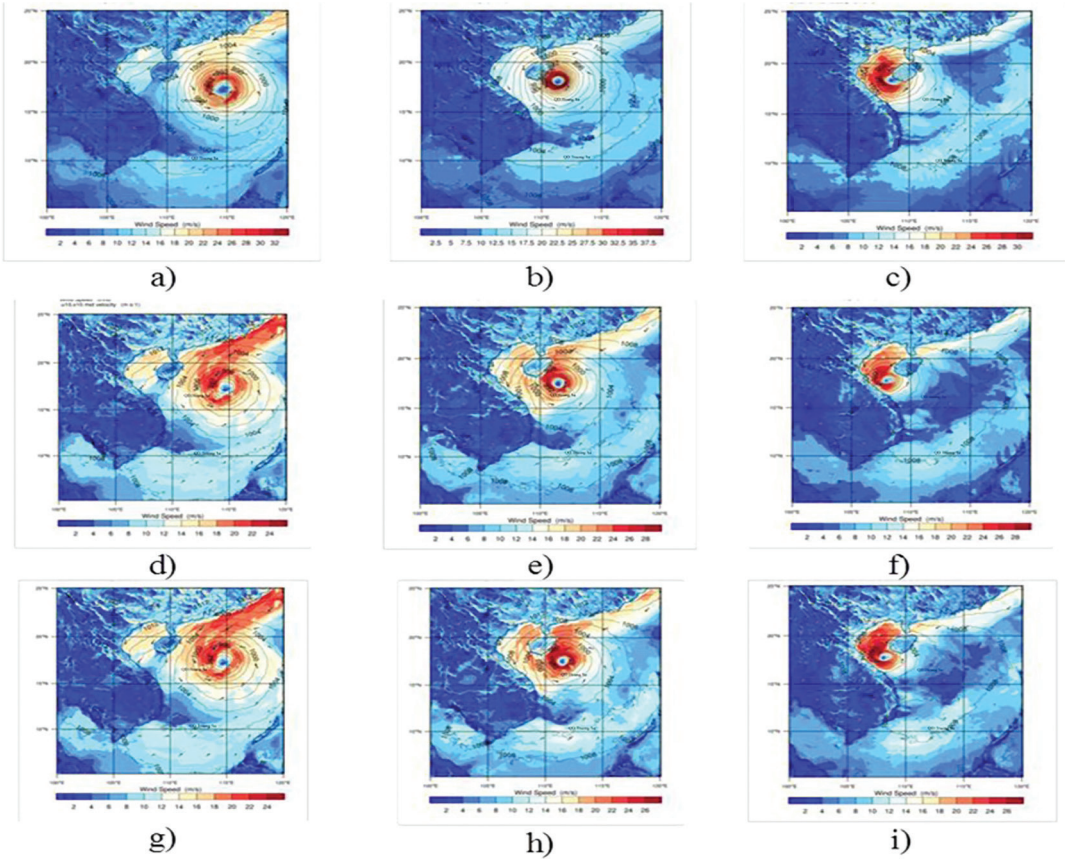

Figure 10. The simulated sea level pressure and the wind velocity at 10 m of Nalgae typhoon after 24 hr (a, d, g), 48 hr (b, e, h) and 72 hr (c, f, i) from 00 Z on October 2, 2011 for: GFS (a, b, c); SSTVT (d, e, f) and SSTUP (g, h, i) cases

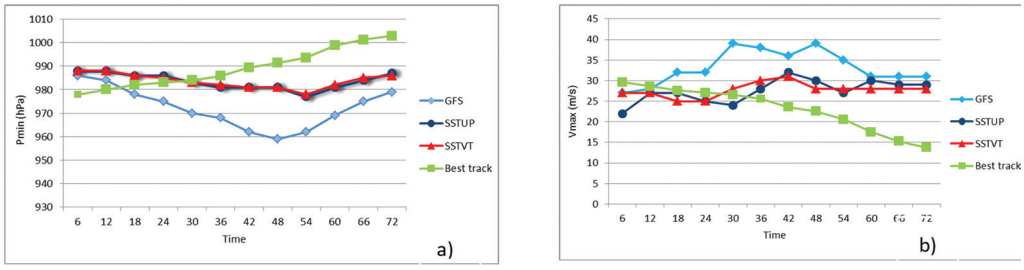

Figure 11. The time series of intensity: a) Pmin; b) Vmax for Nalgae typhoon simulated from 00 Z on October 2, 2011 by GFS, SSTVT and SSTUP cases and observed by IBTrACS (Best Track)

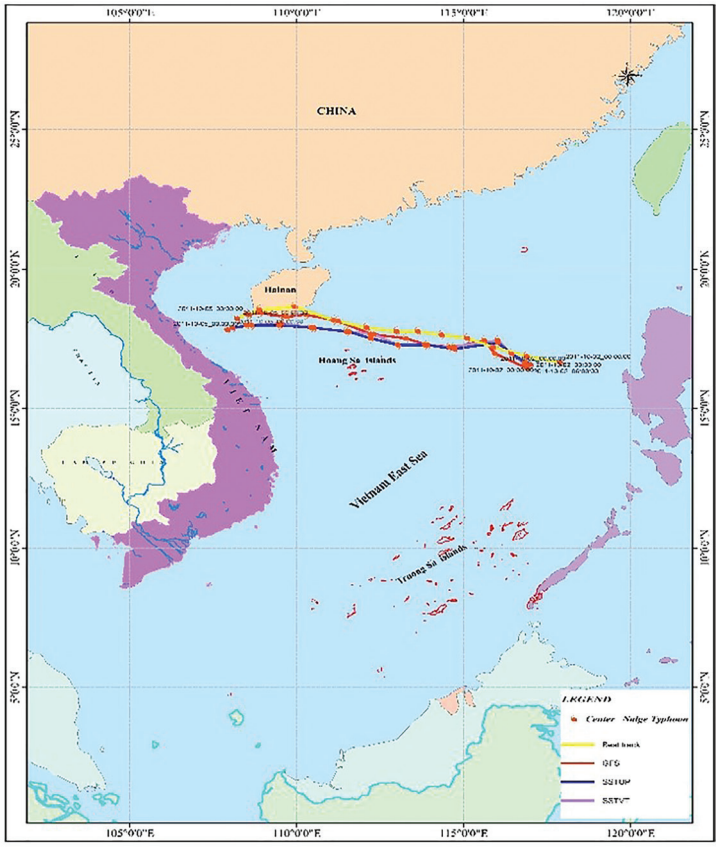

Figure 12. The simulated tracks for Nalgae typhoon from 00 Z on October 2, 2011 by GFS; SSTVT and SSTUP and the observed IBTrACS best track

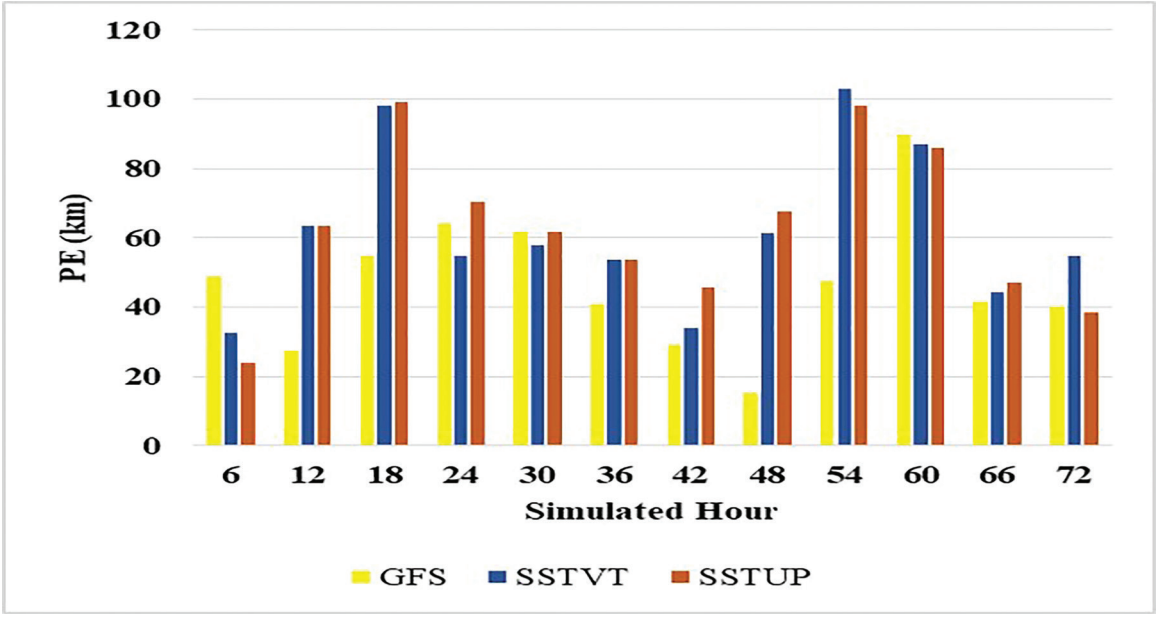

Figure 13. The distance errors (PE) for Nalgae typhoon simulated from October 2, 2011 by GFS; SSTVT and SSTUP cases

4. Conclusion

The present study investigated the effect of SST from satellite data with high resolution of space on intensity and track simulation of typhoon Nalgae (2011). The results demonstrate that the using of SST from satellite data with high horizontal resolution (9x9 km) for both only initial condition case and initial and boundary conditions case plays an important role to improve the 72 hr simulated intensity of typhoon due to improved simulation of latent heat and heat fluxes. The updating of SST for initial and boundary conditions case is not much difference when compared to only initial condition case. The results also show the using of SST from satellite data does not improve the simulated track of typhoon. The further research is required for more reasonable explanations.

References

1. Bright, R.J, Xie, L. and Pietrafesa, L.J. (2002), *Evidence of the Gulf Stream's influence on TC intensity*, Geophysical Research Letters, 29, 1801.
2. Chang and Madala, R. V. (1980), *Numerical simulation of the influence of sea surface temperature on translating tropical cyclones. J. Atmos. Sci.*, 37, 2617–2630.
3. Chen F., Dudhia J. (2001), *Coupling an advanced land surface-hydrology model with the Penn State-NCAR MM5 modelling system*. Part I: Model implementation and sensitivity. Mon. Weather Rev., 129 (4), 569-585.
4. Deepika Rai, S Pattnaik, P. V. Rajesh, and Vivekanand Hazra (2019), *Impact of high resolution SST on tropical cyclone characteristics over Bay of Bengal using model simulations.* Royal Meteorological Society, 26 (1), 130-139.
5. Emanuel, K. (2005), *Increasing destructiveness of tropical cyclones over the past 30 years*. Nature, 436, 686-688.
6. Hong, X, Chang, S.W, Raman, S, Shay, L.K. and Hodur, R. (2000), T*he interaction between Hurricane Opal (1995) and a warm core ring in the Gulf of Mexico. Monthly* Weather Review, 128, 1347-1365.
7. Hong, Song–You, Yign Noh, Jimy Dudhia (2006), *A new vertical diffusion package with an explicit treatment of entrainment processes*. Mon. Wea. Rev., 134, 2318-2341.
8. Iacono, M. J., J. S. Delamere, E. J. Mlawer, M. W. Shephard, S. A. Clough, and W. D. Collins (2008), *Radiative forcing by long–lived greenhouse gases: Calculations with the AER radiative transfer models. J. Geophys. Res*., 113, D13103.
9. Jimenez, Pedro A., and Jimy Dudhia (2012), I*mproving the representation of resolved and unresolved topographic effects on surface wind in the WRF model. J. Appl. Meteor. Climatol.*, 51, 300-316.
10. Kain, John S. (2004), *The Kain–Fritsch convective parameterization: An update. J. Appl. Meteor.*, 43, 170-181.
11. Mandal, M., Mohanty, U.C. MOHANTY, Sinha, P, Ali, M.M. (2007), *Impact of sea surface temperature in modulating movement and intensity of tropical cyclones. Natural Hazards*, 41, 413-427.
12. Miller B.I. (1958), *On the maximum intensity of hurricane. Journal of Meteorology*, 15, 184–185.
13. Palmén E.N. (1948), *On the formation and structure of the tropical hurricane. Geophysical*, 3, 26–38.
14. Shay, G, Goni, J. and Black, P.G. (2000), *Effects of a warm oceanic feature on Hurricane Opal. Monthly Weather Review,* 128, 1366–1383.
15. Shankar, D., Shetye, S.R., Joseph, P.V. (2007), *Link between convection and meridional gradient of sea surface temperature in the Bay of Bengal. Erth Sys Sci*, 116, 385–406.

16. Thompson, Gregory, Paul R. Field, Roy M. Rasmussen, William D. Hall (2008), *Explicit Forecasts of Winter Precipitation Using an Improved Bulk Microphysics Scheme. Part II: Implementation of a New Snow Parameterization. Mon. Wea. Rev*., 136, 5095–5115.
17. Yun, K.S., Chan, J.C.L., Ha, K.J. (2012), *Effects of SST magnitude and gradient on typhoon tracks around East Asia: A case study for Typhoon Maemi (2003), Atmos. Res*., 109, 36–51.
18. Wu, L., Wang, B. and S. A. Braun (2005), I*mpacts of air–sea interaction on tropical cyclone track and intensity. Mon. Wea. Rev.*,133, 3299–3314.

ZONING AGRO-CLIMATIC FACTORS AND EVALUATING ADAPTATION ABILITY OF ARABICA COFFEE IN MUONG ANG DISTRICT, DIEN BIEN PROVINCE

Nguyen Ngoc Anh, Nguyen Huu Quyen, Tran Thi Tam, Duong Hai Yen, Duong Van Kham
Viet Nam Institutes of Meteorology Hydrology and Climate Change

Received: 5 January 2019; Accepted: 18 February 2019

Abstract: *Muong Ang is a mountainous district in the middle of Dien Bien province (the northwest of Viet Nam). Its climatic conditions are quite different compared to the surrounding areas. Specifically, mountainous terrain with a high slope and severe division leads to considerably differentiation in terms of meteorological and hydrological conditions. Muong Ang district is characterised by humid tropical monsoon climate; there are many extreme weather phenomena, e.g. heat wave, unevenly distributed large rainfall, diurnal temperature variation, large seasonal temperature variations. Besides, natural disasters occur quite frequently, such as erosion, landslides, floods and droughts [4]. However, the difference between agricultural meteorology and topography has created a unique landscape in Muong Ang, which is suitable for many kinds of tropical plants with high economic value. Typically, Arabica coffee can adapt very well to the climatic conditions in Muong Ang with high productivity and good quality, which is gradually forming the Muong Ang coffee brand in the domestic and international market.*

In order to confirm the correctness of selecting Arabica coffee to be the main crop in the economic development orientation of Muong Ang district, we need to study the agro-climatic conditions and the agro-climatic zoning of the district and assess the ecological adaptation ability of the coffee in the ecological conditions of Muong Ang, Dien Bien province.

Keywords*: Dien Bien, Arabica coffee, agro-climatic zoning, ecological adaptation, Arabica coffee, Viet Nam.*

1. Introduction

Climate is an irreplaceable component of the living environment. However, the climate is changing towards a detrimental tendency to human and many species. Researching and understanding climate conditions can make the climate invaluable to human life. In relation to agricultural and forestry, the climate is crucially important. Indeed, radiant energy, heat, and water are indispensable climatic factors in creating crop yields and yields. Therefore, the climate is seen as a kind of natural resources. The rational exploitation of climate resource not only provides high and stable crop productivity but also contribute to protecting the ecological environment. In doing so, it is imperative to study the agro-climatic conditions and the agro-climatic zoning

Muong Ang is a mountainous district in the middle of Dien Bien province (the northwest of Vietnam). The district's climatic conditions are quite different compared to the surrounding areas. Specifically, mountainous terrain with a high slope and severe division leads to considerably differentiation in terms of meteorological and hydrological conditions. Muong Ang district is characterised by humid tropical monsoon climate; there are many extreme weather phenomena, e.g. heat wave, unevenly distributed large rainfall, diurnal

Corresponding author: Nguyen Ngoc Anh
E-mail: nguyenanh.imhen@gmail.com

temperature variation, large seasonal temperature variations. Besides, natural disasters occur quite frequently, such as erosion, landslides, floods and droughts. However, the difference between agricultural meteorology and topography has created a unique landscape in Muong Ang, which is suitable for many kinds of tropical plants with high economic value. Typically, Arabica coffee can adapt very well to the climatic conditions in Muong Ang with high productivity and good quality.

Arabica coffee originates from the highlands of southwestern Ethiopia [10]. It accounts for abut 70% of worldwide coffee production. Arabica coffee's optimal temperature range is 18-21^{0}C. It can tolerate mean annual temperatures up to roughly 24^{0}C. The optimal elevation and rainfall for Arabica growth are respectively from 1,300-1,800m (metres above sea level) and from 1,500 to 2,500mm. Coffee can be grown on many different soil types, but the ideal is a fertile, volcanic red earth or a deep, sandy loam. Yellow-brown, high silt soils are less preferred. Avoid heavy clay or poor-draining soils. Coffee prefers a soil with pH of 5 to 6 [4].

In order to confirm the correctness of selecting Arabica coffee to be the main crop in the economic development orientation of Muong Ang district, we need to study the agro-climatic conditions and the agro-climatic zoning of the district and assess the ecological adaptation ability of the coffee in the ecological conditions of Muong Ang, Dien Bien province.

2. Research area

2.1. General geography conditions

The north of Muong Ang district shares the border with Tuan Giao district and part of Muong Cha district. The West is Dien Bien district. The South is Dien Bien Dong district. The East is Tuan Giao district and part of Thuan Chau district (Son La province). Latitude is from 21^{0}24' N to 21^{0}38' N; longitude is from 103^{0}17' E to 103^{0}24' E [10]. Muong Ang terrain is quite complex and divided by high mountain ranges, steep slopes (mostly limestone mountains scattered throughout the area). Located between limestone mountains are narrow and flat valleys. There is not any big river in Muong Ang. Only 4 streams are running through the district, namely Nam Lan, Nam Lich, Nam Co and Nam Ang.

The district has 44,341.2 hectares of natural area and a population of 46,547 people. The rural population include 41,494 people (accounting for 89.1% of the total population of the district) and mainly ethnic minorities. Mostly ethnic minorities are Thai people (78.1%) and Hmong people (11.8%) [8]. The whole district has 9 communes, 1 town and 139 mountainous villages.

2.2. Agro-climatic characteristics in Muong Ang district

Lighting time

Lighting time is assessed through sunny hours. The total number of sunny hours in Muong Ang district is about 2000 hours. The highest number of sunny hours occurs from March to May (about 200 hours/month). The least sunny month is from June to August (130-140 hours/month) [8]. In general, the number of sunny hours in Muong Ang district is quite high compared to other areas in Dien Bien province and the surrounding areas. This condition favour plants that prefer light such as Arabica coffee.

Temperature

The temperature is crucial to the seasonal structure, the time to plant and harvest Arabica coffee. Monitoring data shows that the average annual temperature in Muong Ang district (collected in Tuan Giao station) is about 21.17^{0}C, the coldest month is December (15.9^{0}C), the warmest month is June and July (25.5-25.8^{0}C). The average temperature in January, February, March, November and December is lower than the annual average temperature (21.7^{0}C) [8]. The remaining months have average temperatures higher than the average annual temperature.

Diurnal temperature variation is considered as an important indicator for climate classification. It has a great impact on the growth of plants, especially on the process

of photosynthesis. Due to its location, located in the mainland, Muong Ang has a wide diurnal temperature variation (averaging about 10^0C annually). In the winter (December-March), the diurnal temperature variation is quite dramatic (11-13^{0}C). In summer (June - September), the diurnal temperature variation is about 10.3^{0}C [8].

Absolute minimum temperature

During the winter months, due to the influence of the northeast monsoon, the weather is cold and dry. There often appears sudden weather changes after the cold frontier appearance, the average temperature decreases 3-4^{0}C sometimes 5-6^{0}C. The dry weather at the end of the dry season in the valleys reduces the humidity to below 30%. It is sunny during the light time but it is extremely cold at night time. The strong cooling of the ground facilitates the formation of radiation mist, sometimes frost, especially in the high mountains. Absolute minimum temperature year (-1.2^{0}C) has a great impact on the distribution and growth of Arabica coffee [8].

Rainfall and humidity

The average annual rainfall for many years in Muong Ang district is about 2002mm. Rainfall is unevenly distributed over time and space. Normally, the main rainy season is from April to the end of September. The highest rainfall is distributed in 3 months: June, July and August. It can reach about 200-300mm/month, accounting for 75-92% of the annual rainfall. In the rainy season, the maximum daily rainfall reaches more than 100mm/day, even reaching over 400mm/day [8]. During this period, flooding occurs quite often in low-lying areas. On the sharp slopes of the mountain, it can occur landslides, flash floods, mud and rock floods which results in vegetation loss. The number of rainy days in rainy season is relatively high, about 20 days. The growth of Arabica coffee is badly affected when landslides, floods and flooding occur.

The dry season last for 5 months (November to March) with monthly rainfall under 50 mm/month. However, there are no drought months (rainfall <5 mm/month) [9]. This is a period of shortage of water for coffee trees.

Average annual relative humidity in Muong Ang district is about 80-90%. It varies differently in terms of space and time. The lowest humid months are February and March (about 80%). The highest humid months are July and August (about 87-91%) [9].

2.3. Types of extreme weather

Heatwave (average daily temperature > 35^{0}C)

The average number of hot and sunny days in the period 1962-2017 usually occurs from March to September. The peak months are April and May. Then the number of days slightly decreases from June to September. The highlands have a much higher number of hot and sunny days than the lowlands. The severity of heatwave in the period 1962-2017 (above 35, 37 and 39^{0}C) tends to increase. The increase in the highlands much higher than that in the lowlands. The number of days with temperature above 35^{0}C increased by 6.4 days/decade in the highlands while one in the lowlands did not increase significantly, only 1.4 days/decade. The number of days with temperature above 39^{0}C has markedly fluctuated by years in the highlands, but the increase is negligible [9].

Extreme cold (average daily temperature ≤ 15^{0}C) and damaging cold (average daily temperature ≤ 13^{0}C)

The cold weather in the period of 1962-2017 usually occurs from November to March. The peak is usually in January and February. The difference between the highlands and lowlands is very small. The highlands appear to be cold more often than the lowlands (about 1 to 2 days). There is a huge fluctuation in the number of extreme cold and damaging cold days in the period 1962-2017. It can reach over 40 days of extreme cold in some years and be only 5 days in some other years. The average number of damaging cold days is about 5 days/year, and up to 12 days/year in some years. In general, extreme cold and damaging cold tend to decrease. However, the number of extreme cold days in the highlands tends to increase slightly, less than 1 day/decade.

Heavy rain (number of days with rainfall greater than 50 mm)

During the period of 1962-2017, heavy rain usually occurred from April to September, peaked in June-August. The lowland areas often have a larger number of rainy days than that in the highlands. The maximum daily rainfall is from 200 to 600mm, usually occurs from May to August (July is the largest value) [9]. The highlands have an average rainfall of 50-200mm. There is a large difference between locations regarding the number of heavy rainy days in the years: the highlands with 10 days, the lowlands with 16 days. In addition, there is a huge variation in extremely high rainfall between years, ranging from 100mm to 600mm [9]. The lowlands often have this value greater than that of the highlands. However, there is no significant difference in relation to extremely high rainfall in the year between high and low areas.

2.4. The other special weather phenomena

Foehn wind effect, fog, hoarfrost, thunderstorm and hail often occur in the district. They significantly affect the life and health of the people in Muong Ang.

Hail appears almost every year in Muong Ang during the end of winter and beginning of summer. It is 0.2-0.6 days occurs hail every year. Hail mainly appears from February to May. Hail damages the coffee gardens that causes broken branches, flowers and fruits, etc. and could completely destroy the crop. Hail is classified as a dangerous weather phenomenon.

Fog often occurs in the district with uneven distribution depending on the local terrain characteristics. The number of foggy days is about 90 days per year and usually occurs during the winter months, especially in December, January and February. This is also a dangerous weather phenomenon because it can cause coffee plants to die.

Muong Ang often appears thunderstorms. Thunderstorms with strong winds often cause significant damage to local people. On average, there are 70-90 thunderstorms each year. Thunderstorms often appear in April - August with about 6-15 days/month [9]. The thunderstorms here are not serious but can be accompanied by strong winds and hail during the transition period from spring to summer.

It is quite common for the phenomenon of foehn winds. In the lowlands (<500m), there are about 5-30 days of foehn winds per year. The higher it is, the fewer the number of hot and dry days. Hot and dry weather often occurs in the period of February to September, mostly in April and May [9].

3. Data and research methods

3.1. Data

Meteorological data

Meteorological data in Muong Ang district and surrounding areas were collected at 6 meteorological stations including Dien Bien, Tuan Giao, Pha Din, Son La, Song Ma and Lai Chau in the period 1961-2017. The representative data was collected at Tuan Giao station due to the fact that this station shares similar natural conditions to Muong Ang district. The data system is summarized in Table 1 and Figure 1.

Remote sensing data

Muong Ang is one of the mountainous districts of Dien Bien Province. Its terrain characteristics reflect a complex division. A high slope and severe division lead to considerably differentiation in terms of meteorological and hydrological conditions. Therefore, in order to increase the objectivity and scientific foundation for analysis, it needs to supplement the temperature and humidity data interpolated from MODIS and NOAA satellite images in the period of 2000-2018. In addition, data and trends of temperature, precipitation, humidity and atmospheric pressure in the different areas of Muong Ang can be accessed through the website [10].

Survey data on the current state of agricultural production

Field survey to collect documents and data related to agricultural production includes seasonal structure, cultivated area, productivity, output, land use map, soil distribution map, the status quo of natural disasters and epidemics in

Muong Ang district. These documents and data are then used for the assessing and classifying agro-climatic zones in Muong Ang district.

Other data

Documents for establishing single maps, maps of agro-climatic zones we collected from the national database provided by the Ministry of Natural Resources and Environment - the maps detailed at commune levels with the scale of 1: 25,000.

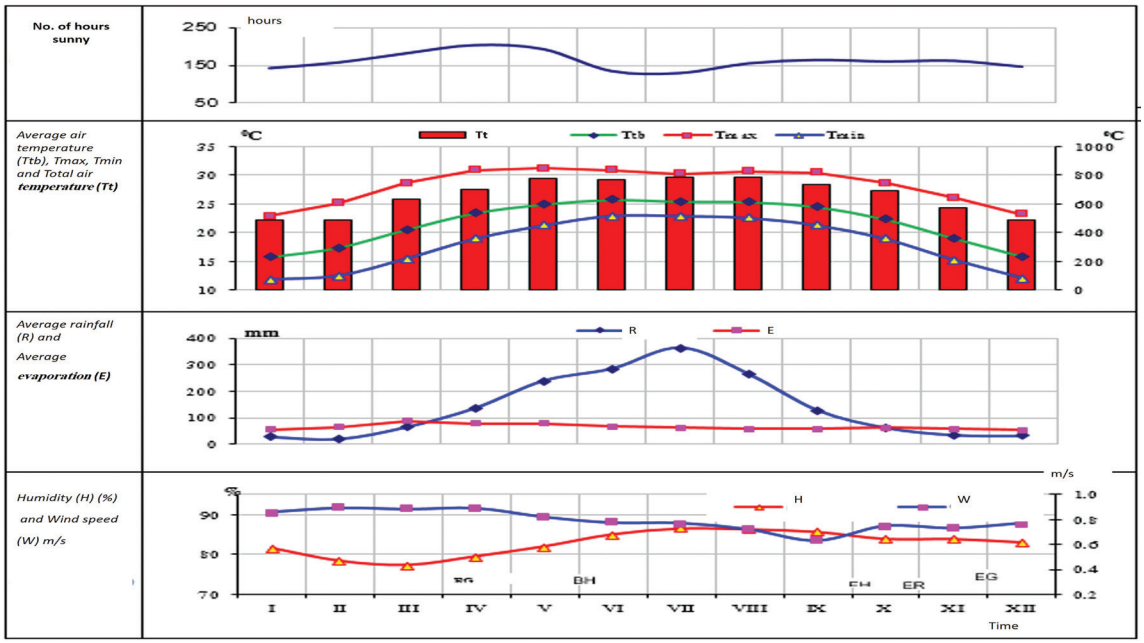

Figure 1. Climate condition graphs of Muong Ang district at Tuan Chau station, 2017.

Table 1. Meteorology climate data in Muong Ang district

Climate factor	Months												Year
	I	II	III	IV	V	VI	VII	VIII	IX	X	XI	XII	
Average temperature	15.7	17.4	20.5	23.4	25.0	25.8	25.5	25.4	24.5	22.4	19.1	15.9	21.7
Temperature range	11.1	12.7	13.2	12.0	9.9	7.9	7.3	8.1	9.1	9.8	10.8	11.1	10.3
Lowest temperature	10	12	14	18	19	22	22	22	20	17	14	10	10
Number of cold days	4.4	2.7	0.4	0.1	0.0	0.0	0.0	0.0	0.0	0.0	0.6	4.4	1.1
Number of sunny hours	141.2	156.8	182.1	204.5	193.6	133.4	127.8	154.3	163.8	159.5	161.5	145.3	1923.8
Average rainfall	29.4	21.3	66.4	137.5	239.6	285.0	363.1	263.0	128.5	63.1	36.0	33.1	138.8
Number of rainy days	18.0	4.5	4.1	7.0	12.6	17.8	21.5	23.8	20.5	13.2	7.7	5.4	-
Relative humidity	82	78	77	80	82	85	87	86	86	84	84	83	83

Source [9]

3.2. Research Methods

3.2.1. Calculating values

The degree of change:

Determining the average value $\left(\overline{x}\right), \overline{x} = \frac{1}{n}\sum_{t=1}^{n} x_t$

Determining the maximum value (Max and Min) by filtering Max_{xt}= Max (x_1, x_2,...x_n); Min_{xt} = Min (x_1, x_2,...x_n); In which t is the time series (t = 1, 2, ..., n-1, n); x_t is a series of data observed over time ($x_t = x_1, x_2, ..., x_{n-1}, x_n$).

The trend of change

The tendency of changes in past climate factors is often assessed by identifying (a) in the regression line equation:

$X = a_0 + a_1 t$. In which, X is calculated from the series of observational data over time (x_t); t is the time series (can be month, year, decade, etc.), a0 is the cutting coefficient, a1 is the corner coefficient. If $a_1 > 0$, the tendency is to increase, if $a_1 < 0$ then the tendency is to decrease.

Revising the reliability of the correlation coefficient

The correlation coefficients is often used in climate research to provide objective conclusions regarding the correlation relationship between variables provided the following formula to revise the reliability of the correlation coefficient [5]:

$$-t_{\frac{a}{2},n-1} S_r < r_k < t_{\frac{a}{2},n-1} S_r$$

with $S_r = \frac{1}{\sqrt{n}} - t$

r_k is the correlation coefficient between two chains; S_r is the standard error of the autocorrelation coefficients r_k; α is the value in the object distribution with n-1 degrees of freedom. In climate research, normally α is 0.01 or 0.05 [7].

Interpolation of temperature and rainfall distribution

Based on the average monthly air temperature data in the period 2001-2017 collected at 6 meteorological stations (T_obs) and the surface coating temperature value (LST) were analyzed by image data (MOD11A2), which were set up at the same time and same location. The relationship between T_obs and LST with sample size n = 72 (12 months x 6 stations) is used to interpolate the temperature distribution for Muong Ang district and surrounding areas..

Similarly, the total annual rainfall is interpolated. Used data includes the average monthly rainfall value collected 6 stations (R_obs) in the period 1981-2017 and the rainfall from the CHIRPS data set (R_Chirps).

3.2.2. Method of classifying agro-climatic zones

The agro-climatic zones of Muong Ang district were classified in 5 steps:

Step 1: Determining the partition criteria. The total annual heat index indicates the degree of tolerance of the climate to plants. It also reflects the annual temperature range and related natural disasters (e.g. heat wave, extreme cold). Normally, the total annual temperature is usually proportional to the average seasonal temperature and the number of warm and sunny days while it is inversely proportional to the number of cold days.

Step 2: Determining boundaries between the zones based on the isothermal lines 8500^{0}C (D.V. Kham et al. 2012). The areas with total temperature higher than 8500^{0}C and average elevation under 100m are called 'lowlands'. The areas with total temperature lower than 8500^{0}C and average elevation higher 100m are called 'highlands'. The terms 'low and highlands' are often used by local people. Determining the boundary between sub-zones based on the 2000mm isometric line with the distance between the isosceles lines is 500mm [7].

Step 3: Overlay the maps. The thematic maps (precipitation, temperature, topography, slope, traffic, waterways and administrative boundaries at commune level) are overlapped using GIS technology. The map of agro-climatic zones was established are in lines with the VN2000 reference system, the international UTM projection grid, Ellipsoid WGS84 adapted to Viet Nam [2]. The map was established at the scale 1:50,000.

Step 4: Designing map legend.

Step 5: Edit and finalize the map consulting experts and local officials [1],[7].

3.2.3. Evaluating cultivation potential in agro-climatic zones and sub-zones

The evaluation was based on the instruction of FAO's soil assessment which is coded in the LUSET model [1],[7]. The model consists of two modules: module 1 is for inputing data related to the plants and soil; module 2 is for processing and outputing data.

Using GIS technology to divide Muong Muong district into land units (LU) with a resolution of 100x100m resulting 44,515 LU. In order to assess the relevance of each LU regarding the needs of different crops, the information in each identified LU must reflect similar information to the needs of the crops. Climate data including average monthly temperature and monthly rainfall are interpolated for each LU. Slope data is calculated from topographic maps (DEM). Soil data is determined from the soil map and encoded according to the unit system required by the LUSET model. The identified soil characteristics referencing to ecological requirements of arabica were interpolated for determining suitable areas for Arabica. The outputs of the LUSET model are integrated with the agro-climatic zones map (Figure 2).

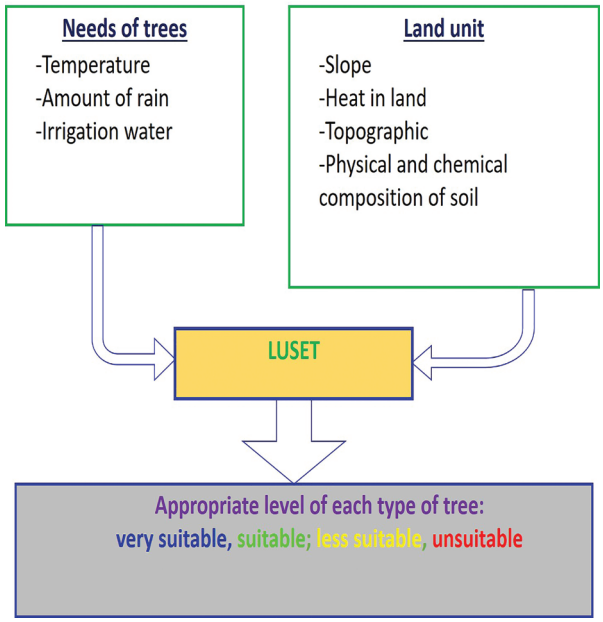

Figure 2. Process of determining the cultivate potential in agro climatic sub-zones, Source [1, 2]

Selecting a calculation method

Select a calculation method

Based on the needs of the crop and the factors related to soil, temperature, and water resources in each LU, the LUSET model can calculate the suitability (OVS) for each element and integrated elements into index synthesized OVS through 4 methods: Minimum, Maximum, Average and Redundant so that users can choose an appropriate method depending on the purpose of use. Natural disasters often occur in Muong Ang, e.g., heavy rain, flooding, heat wave, droughts, cold and extremely cold weather. In addition, agricultural production has not been developed. Most of the cultivated area strongly depends on rain. Therefore, the method selected is "Minimum". This is the assessment method with the highest safety level among the four methods. Appropriate index is defined as the lowest score of all factors considered. OVS is calculated according to the formula:

OVS = Min (SF1, SF2, SF3,... SFn). In which: OVS is the appropriate value; SF1, SF2, SF3,... SFn is the appropriate score (ranging from 0 to 100) of the n selected elements.

The calculation of OVS index is done in 2

steps.

Step 1: Calculating OVS separately for each element (OVSg), OVSg can be soil (slope, soil depth, soil type), temperature (average temperature per month) or water (monthly rainfall, assumed irrigation or not).

OVSg = f (S1, S2, ..., Sn).

S1, S2, ... Sn are the appropriate score of elements in a group; f is a function to calculate the overall suitability (Min function).

Step 2: Calculating the overall fit from three groups of factors (soil, temperature, water).

OVS = f (Ss, Sh, Sw). In which: Ss, Sh, Sw are OVSg values corresponding to soil, temperature and water element.

The scores and weights in calculating OVS index:

Due to the different ecological characteristics of each crop, the role of each element in the crop is different. Therefore, determining the appropriate score for an element is divided according to the weights from 1 to 3 (1 is the most important, then 2 and 3). This study uses FAO weighting sets [1]. The score for the 4 appropriate levels corresponds to the three weights shown in Table 2.

Table 2. Appropriate levels corresponding to the weight factors [7]

Suitability levels	weight number = 1	weight number = 2	weight number = 3
S1	85	95	100
S2	60	65	70
S3	40	45	50
S4	0	10	15

Combining the appropriate elements and weighting factors to create a value that ranges from 0 to 100. This value is the OVS score of the elements considered for a particular crop in a LU. Using the minimum method to determine an overall suitable value and then to classify the suitability levels from S1, S2, S3 to N (Table 3).

Table 3. Classification of overall suitability [7]

No	Score	Suitability levels	Legend
1	≥ 85	S1	Very suitable
2	≥ 60 and < 85	S2	Suitable
3	≥ 40 and < 60	S3	Less suitable
4	< 40	N	Not suitable

Calculating the cultivation potential area in the zone and sub-zones: Based on the adaptive conditions of Arabica coffee, the map ecological adaptive ability was built.

Applying GIS technology with Krigging method - distance inversion algorithm (IDW) in spatial interpolation and overlaying information level to establish thematic maps.

4. Results

4.1. Classifying agro-climatic zones in Muong Ang

The climate and agro-climatic climate are decisive in forming agricultural production areas. Therefore, classifying agro-climatic zone is a scientific basis for rational distribution of crop structure. It helps to classify agro-climatic zones and sub-zones based on climatic features and the conditions of agricultural production. The map of agro-climatic zones is the scientific basis for many purposes. For example, planning agricultural and forestry production; assessing the adaptation of crops in general and Arabica coffee in particular; assessing water resources; assessing the impact of climate change on people's lives and production; helping people identify appropriate cultivation measures; calculating potential yield of crops in regions and sub-regions; determining the structure of crops.

4.1.1. Identifying agro-climatic sub-zones in Muong Ang district

- *Criterion 1*: The first indicator to delineate the agro-climatic sub-regions is the total annual temperature. The total amount of temperature in a year is directly related to the annual average temperature and somehow related to the annual variation of temperature. The annual variation of temperature indicates the thermal season, the growing season of plants. This is the foundation for determing planting/harvesting seasons.

- *Criterion 2*: Total annual rainfall is important to the growth of crops, especially Arabica coffee in Muong Ang where the irrigation water depends mainly on rainwater. This indicator is used to assess the available water supply for agricultural production and then for selecting rational crops structure and proposing appropriate irrigation solutions.

- *Criterion 3:* Temperature decreases with increase in altitude.

- *Criteria 4*: the reduction of rainfall according to the terrain, wind direction, air masses with high moisture content.

Synthesizing the above criteria to classify agro-climatic zones. The results are presented as follows:

- Thermal background of the district is divided into 4 thermal zones as shown in Figure 3:

+ Zone T1 (elevation above 1,500m): Total annual temperature is below 7,000^{0}C, the annual average temperature is below 20^{0}C. This region is located in the northwest of Muong Dang commune, east of Xuan Lao commune, south of Cang Cang commune and Nam Lich.

+ Zone T2 (800-1,500m): Total annual temperature is from 7,000-7,500^{0}C, annual average temperature is from 20- 21^{0}C. This area is mainly concentrated in the northern edge, west and south of the district.

+ Zone T3 (600-800m): Total annual temperature is from 7,500-8,000^{0}C, the annual average temperature is from 21-22^{0}C. This region accounts for the largest portion and is distributed in most communes in the district.

+ Zone T4 (lowlands, valleys along rivers and streams, altitudes from 400-600m): Total annual temperature is from 8,000-8,500^{0}C, the annual average temperature is over 22^{0}C. This area is distributed along the valley of rivers and streams in Ang To, Bung Lao, Xuan Lao and Muong Lan communes.

- The number of sunny days in the district is divided into 4 sub-regions on the map of Figure 4. The map shows that the number of sunny days (over 35^{0}C) with the value over 15 (days) occupies a fairly wide range in the whole district. Overall, Muong Ang receives a large amount of heat, concentrating on the district centre. In the edge of the district, the number of sunny days gradually decreases. This is an important basis for the district to make appropriate crop structure choices.

- The number of cold days in the district is shown in figure 5 with 4 areas. The areas featuring the number of cold days at over 25 days include the highlands of Xuan Lao commune, south of Ang Cang commune, and west and northwest of Muong Dang commune. The remaining areas have a number of cold days less than 15 days.

- The humidity in Muong Ang is presented in Figure 6.

+ Zone R1: Total annual rainfall is over 2,000mm. This area is located in a mountainous area (>1,000m) in the northwest of Muong Dang commune. It is easy to happen flash floods when it has unusually heavy rain. This is a remote area for people to access and develop agriculture and forestry. Therefore, forest in this area is preserved quite well and it is difficult to grow Arabica coffee here.

+ Zone R2: Total annual rainfall from 1,900 to 2,000mm. This area is distributed in mountainous areas with an altitude of 800-1,000m, belonging to communes of Coong Cay, Muong Dang, Ang Nua, Ang Cang and Nam Lich.

+ Zone R3: Total annual rainfall from 1,800-1,900mm. This region is distributed in areas with elevations between 600-800m, belonging to communes in the central area to the west of the district.

+ Zone R4: Total annual rainfall is less than 1800 mm. This region is distributed in eastern communes of the district.

- The annual average number of heavy rainy days in the district is shown in Figure 7. Mostly areas of two communes of Cang Cang and Ang Nưa belong to the region with few heavy rainy days (2-3 days). This is a positive indicator for the development of Muong Ang Arabica coffee. Through the map of Figure 7, it is found that the annual average number of heavy rainy days is concentrated in the edge of the district such as the easternmost area of Xuan Lao commune,southwest and south of Phung Cang commune, North and Northwest of Muong Dang commune. The central part of the district has less rainy days than the outer border.

4.1.2. The map of agro-climatic zones

Most of the district's area is hilly and mountainous in different directions and with highly differentiated elevations. This is the reason why the district has many sub-zones (6 sub-zones) as shown in Figure 3. This map is the final result of the process of researching, analysing and evaluating climate conditions for the purpose of classifying agro-climatic zones of the district.

Temperature variation of the sub-zones is visualized in the diagram in Figure 3,4.

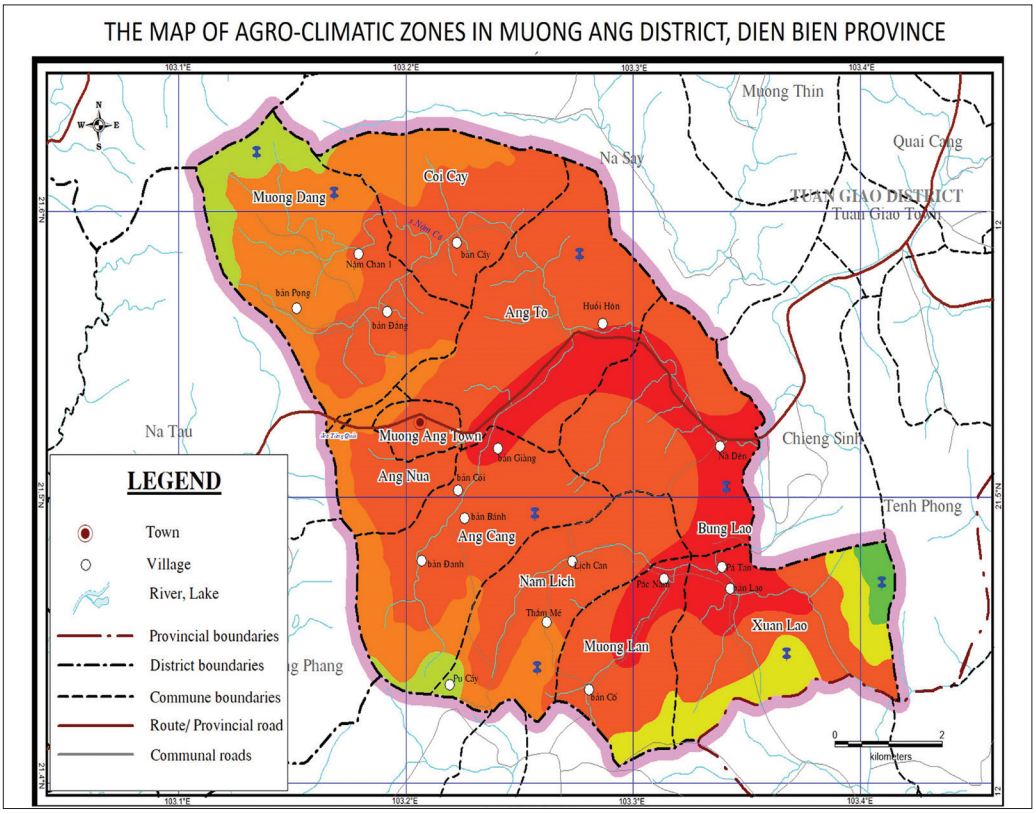

Figure 3. Map of Agro-climatic zoning

The diagram shows that the temperature in the sub-zones is quite consistent and in line with a rule. The sub-zones all reach their maximum temperature in June and minimum in December and January. The temperature differentiation is also consistent with the space distribution of the sub-zones. This explains the correctness of the analysis.

The rainfall of the sub-zones is also quite uniform. Rainfall is highest in July and gradually decreases in November, December, and January. Rainfall is minimum in February.

- Sub-zone 1: the total annual heat below 7,000^{0}C, the annual average temperature is under 20^{0}C; Total annual rainfall is from 1,800-1,900mm. The average number of hot and

sunny days (T>35^{0}C) is about 5days per year; the number of extremely cold days (T<15^{0}C) is about 45-60 days/year; the number of damaging cold days (T≤13^{0}C) is about 25-35 days/year; the number of days with heavy rain (R>50mm) is about 3-4 days/year. This sub-zone is distributed at the eastern edge of Xuan Lao commune.

- Sub-zone 2: The total annual heat, temperature and average number of hot sunny days are the same Sub-zone 1; The total annual rainfall is greater than or equal to 1,900mm. the number of extremely cold days is from 30-45 days/year; the number of damaging cold days is about 15-25days/year; the number of days with heavy rain is about 3-4 days/year. This sub-zone is distributed in the northwest of Muong Dang commune and a small part of the mountain area above 1500m in Ang Cang commune and Nam Lich.

- Sub-zone 3: The total annual temperature from 7,000-7,500^{0}C, the annual average temperature of 20-21^{0}C; Total annual rainfall is under 1,800mm. The average number of hot sunny days is similar Sub-zone 1. The number of extremely cold days is about 30–45 days/year; the number of damaging cold days is about 15-25days/year; the number of days with heavy rain is about 2-3 days/year. This sub-zone is mainly distributed in the highlands above 800m in Xuan Lao and Muong Lan communes.

- Sub-zone 4: This sub-zone is the same Sub-zone 3 by heat, temperature, extremely cold days, damaging cold days and heavy rain day. There is a different at the total annual rainfall is from 1,900 to 2,000mm. The average number of hot and sunny days is about 5-10 days/year. This sub-zone is mainly distributed in areas with elevations below 1,000m in the northern edge, west and south of the district.

- Sub-zone 5: The total annual temperature from 7,500-8,000^{0}C, the annual average temperature of 21-22^{0}C; Total annual rainfall is from 1,800 to 1,900mm. The average number of hot and sunny days is 10-15 days/year; the number of extremely cold days is about 15-30 days/year; the number of damaging cold days is about 6-15 days/year; the number of days with heavy rain is about 1-2days/year. This sub-zone is mainly distributed in the area of 600-800m belonging to most communes in the district.

- Sub-zone 6: The total annual temperature higher than 8,000^{0}C, the annual average temperature higher than 22^{0}C. Total annual rainfall is less than 1,800mm. The average number of hot and sunny days is higher than 15 days/year; The number of extremely cold days, damaging cold days and heavy rain day are similar the sub-zine 5. This sub-zone is mainly distributed in areas with elevations below 600m and river valleys in Ang To, Bung Lao, Xuan Lao and Muong Lan communes.

Table 4. The legend for Agro-climatic zone

Region	Sub-region	Symbol	Total heat (oC)	Tavr (oC)	Total rainfall (mm)	Characteristics of adverse weather conditions
Highland	Sub-region 1		< 7000	< 20	1800 - 1900	Hot and sunny day (>=35 celsius) appears about 5 days/year for sub-region 1,2,3; 5-10 days/year for sub-region 4; 10-15 days/year for sub-region 5 and over 15 days/year for sub-region 6 Strong cold day (<=15 celsius) appears about 60-80 days/year for sub-region 1; 45-60 days/year for sub-region 2; 30-45 days/year for sub-region 3,4 and 15-30 days/year for sub-region 5,6. Harmful cold day (<=13 celsius) appears about 35-50 days/year for sub-region 1; 25-35 days/year for sub-region 2; 15-25 days/year for sub-region 3,4 and 6-15 days/year for sub-region 5,6. Heavy rain day (>=50 mm) appears about 4-5 days/year for sub-region 1; 3-4 days/year for sub-region 2; 2-3 days/year for sub-region 3,4 and 1-2 days/year for sub-region 5,6.
	Sub-region 2				>=1900	
	Sub-region 3		7000 - 7500	20 - 21	< 1800	
	Sub-region 4				1900 - 2000	
Lowland	Sub-region 5		7500 - 8000	21 - 22	1800 - 1900	
	Sub-region 6		> 8000	> 22	< 1800	

On the website https://www.meteo-blue.com, extract values of temperature and precipitation corresponding to the location of sub-regions on the map of agro-climatic zone in Muong Ang, to determine the interplay of temperature and rainfall. The results are reflected in the graphs shown in Figures 4, 5 [10]:

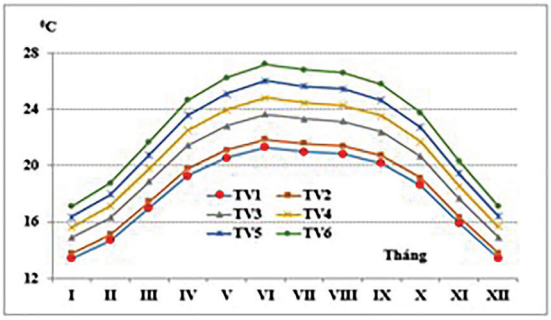

Figure 4 . Temperature variation in sub-zones

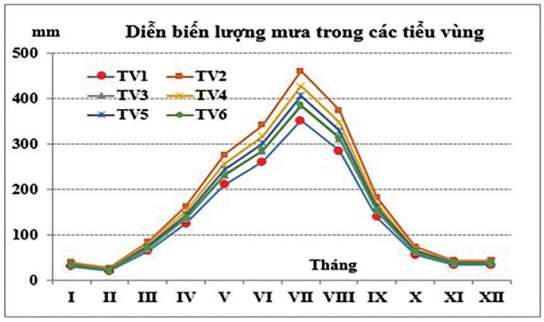

Figure 5. Rainfall variation in sub-zones

Through the diagrams in Figures 1, 4, 5 and the map on Figure 3, the high compatibility between the partition results, the actual monitoring data at Tuan Giao station and the information extracted from the website.

The application of GIS and remote sensing technology to build a map of the agricultural climate zone is an important achievement and a new scientific product for socio-economic planning and development at Muong Ang district, Dien Bien province.

4.2. Classifying zones depending on ecological adaptation of Arabica coffee

Ecological and growth characteristics of Arabica coffee is analyzed carefully for interpolating ecological adaptation. The result is shown in Figure 6. The map shows that the coffee can adapt very well in sub-zones 4, 5 and 6. Sub-zones 1, 2 and 3 are not suitable for planting the coffee [4]. Based on the map, data on the area of adaptive levels can be extracted (Table 5 and Figure 7).

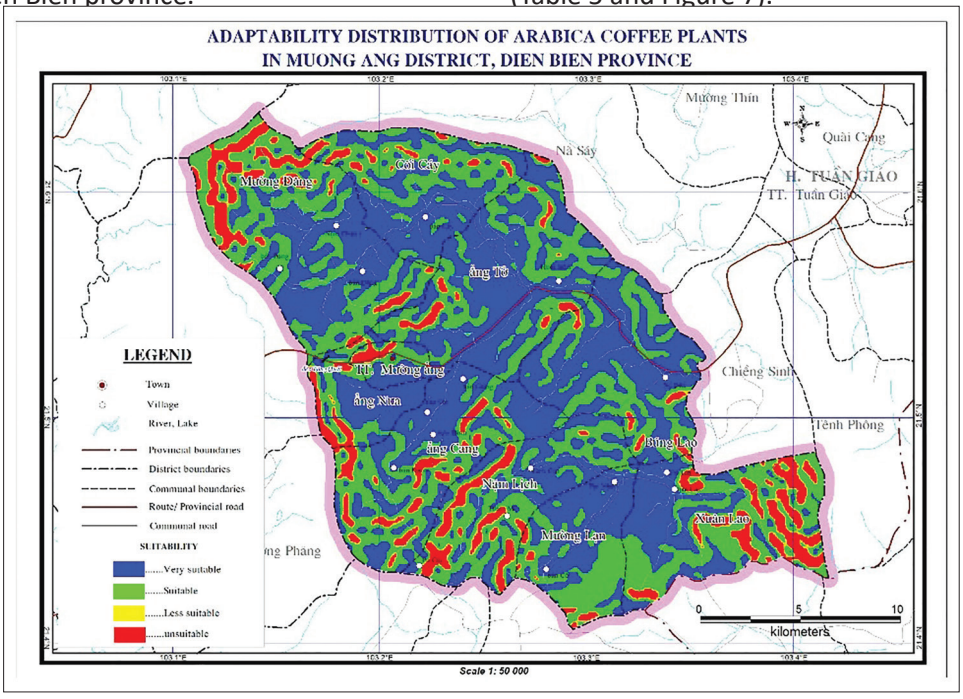

Figure 6. Map of ecological adaptation of Arabica coffee in Muong Ang district

The area and productivity of Arabica coffee in Muong Ang are presented in Table 6.

In 2017, after applying the results of scientific research into the production process, the output of Arabica coffee in Muong Ang increased significantly from 4,965 tons (in 2013) to 7,244.9 tons (in 2017). In the meanwhile, the area for planting decreased slightly. This confirms the effectiveness of agricultural development in the district.

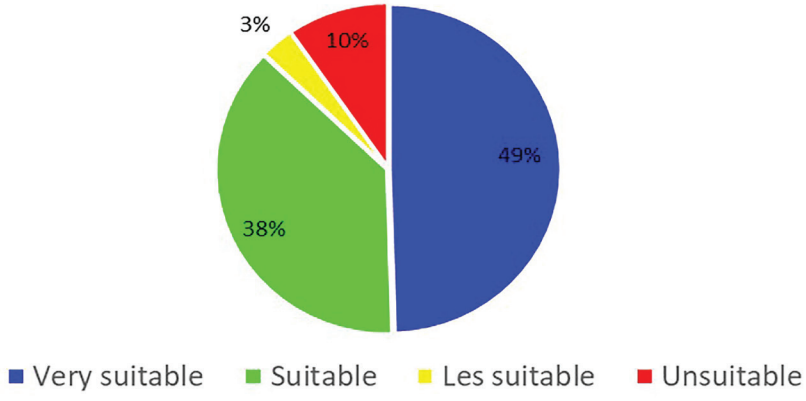

Figure 7. Structural levels of the ecological adaptation of Arabica coffee trees

Table 5. Soil structure by adaptive capacity of Arabica coffee

Levels	Area (ha)	Proportion (%)
Very suitable	21,955.77	49.52
Suitable	16,703.18	37.67
Moderate	1,416.44	3.19
Unsuitable	4,266.06	9.62

Table 6. Area and production of Arabica coffee in Muong Ang district [8]

Year	2013	2014	2015	2016	2017
Planting area (ha)	3,318.2	3,349	3,428	3,449.3	3,311
Area for harvesting (ha)	1,655	1,951	2,999	3,200	3,154.1
Coffee production (ton)	4,965	3,200	5,700	3,094	7,244.9

5. Conclusion and recommendations

The agro-climatic zone of the district is divided into 6 sub-zones based on the criteria of temperature, rainfall, humidity and algorithms and spatial interpolation methods. This research aims at serving the crop selection, planning and, most importantly, socio-economic development planning of Muong Ang district.

The communes selected for the pilot study include Ang Nua and Ang Cang. In which, Ang Nua commune is in sub-zones 4 and 5, Ang Cang commune is located in sub-zones 2, 4 and 5. The area of sub-zone 2 of Ang Cang commune is quite small. Both communes share quite a similar agro-climatic condition.

Sub-zones 4 and 5 are the most beneficial for growing industrial crops and perennial crops, typical Arabica coffee, citrus fruit, longan, plum and cashew. Annual crops should be corn and peanuts. Rice is slightly adaptable.

Still there exist some shortages in this research:

+ Due to the fact that there is no monitoring station in Muong Ang district, the data for analysis is collected in a neighbouring station (Tuan Giao station) and interpolation data from satellite images and GIS. This affects

the accuracy of the results. However, the result is still acceptable.

+ When establishing ecological adaptation maps of some main trees, it lacks a number of soil criteria such as soil thickness, pH, chemical components in the soil. It is for the reason that the there is no available data in the district. However, thanks to other criteria such as temperature, precipitation, humidity, experience and expert knowledge, the findings are highly reliable.

We have some recommendations as follows:

- It is imperative to build a monitoring station in Muong Ang district. It can be located in Ang Nua commune or Yen Cang commune to monitor and provide data for the whole district serving researching, planning and for other research-related purposes.

- The district should establish a soil map system with a scale of 1: 50,000 or more detailed in order to identify accurately soil characteristics serving agricultural and forestry production.

- Expanding research areas for other communes regarding interdisciplinary development throughout the district.

References

1. Bernardi M., (2000), *Application software developed by FAO for management of soils and crops data*. Software for Agroclimate data management. USDA & WMO.
2. Huard F. and Perarnaud V., (2001), *Agrometeorological database management strategies and tools in France*. WMO & USDA.
3. Jagtap, Shrikant S., (2001), *Planning sustainable agriculture using agroclimatic database.* WMO - CAgM.
4. Mitchell, H. W. (1988), *Cultivation and Harvesting of the Arabica Coffee Tree*. Book.
5. Oldeman L.R., Frere.M (1998), *A study of the agroclimatology of the humid tropics of South East Asia*. FAO/UNESCO/WMO No.597, 230p.
6. Stigter C.J., Das H.P., J.J. Salinger. (2000), *Agrometeorological adaptation strategies to increasing climate variability and climate changes*. WMO-CagM.
7. CARE Viet Nam (2018), *Developing an agro-climatic zoning map in Muong Ang district - Dien Bien province*. PR1711_VNM257 ACIS.
8. Dien Bien's Statistics Department (2018), *Statistical Yearbook of Dien Bien Province. Statistical Publishing House.*
9. General Department of Meteorology and Hydrology (2017), *Set of meteorological and hydrological data.*
10. https://www.climate.gov/news-features/climate-and/climate-coffee.
11. https://www.meteoblue.com.
12. http://www.dienbien.gov.vn.